

LEVERAGING MULTI-TIME HAMILTON-JACOBI PDES FOR CERTAIN SCIENTIFIC MACHINE LEARNING PROBLEMS

PAULA CHEN^{*‡}, TINGWEI MENG^{†‡}, ZONGREN ZOU^{*‡}, JÉRÔME DARBON^{*§}, AND GEORGE EM KARNIADAKIS^{*}

Abstract. Hamilton-Jacobi partial differential equations (HJ PDEs) have deep connections with a wide range of fields, including optimal control, differential games, and imaging sciences. By considering the time variable to be a higher dimensional quantity, HJ PDEs can be extended to the multi-time case. In this paper, we establish a novel theoretical connection between specific optimization problems arising in machine learning and the multi-time Hopf formula, which corresponds to a representation of the solution to certain multi-time HJ PDEs. Through this connection, we increase the interpretability of the training process of certain machine learning applications by showing that when we solve these learning problems, we also solve a multi-time HJ PDE and, by extension, its corresponding optimal control problem. As a first exploration of this connection, we develop the relation between the regularized linear regression problem and the Linear Quadratic Regulator (LQR). We then leverage our theoretical connection to adapt standard LQR solvers (namely, those based on the Riccati ordinary differential equations) to design new training approaches for machine learning. Finally, we provide some numerical examples that demonstrate the versatility and possible computational advantages of our Riccati-based approach in the context of continual learning, post-training calibration, transfer learning, and sparse dynamics identification.

Key words. Multi-time Hamilton-Jacobi PDEs; Hopf formula; machine learning; linear quadratic regulator; linear regression; Riccati equation

1. Introduction. It is well-known that Hamilton-Jacobi partial differential equations (HJ PDEs) have deep connections to optimal control [1], differential games [12], and imaging sciences [5, 9], among many other fields. When the Hamiltonians are convex and only depend on the momentum, the solution to the HJ PDEs can be represented by a Hopf formula, which converts the solution of the PDE to the solution of an optimization problem. Multi-time HJ PDEs were originally introduced in economics [29]. The solution to certain multi-time HJ PDEs was then shown to be able to be represented by a multi-time Hopf formula [22], which is a generalization of the single-time case and has been shown to have connections with imaging sciences [8].

In this paper, we establish a novel theoretical connection between certain optimization problems arising in machine learning and the multi-time Hopf formula (Section 2). Specifically, we show that there are one-to-one correspondences between the loss functions in certain learning problems and the objective function of the multi-time Hopf formula, which in turn yields connections to certain optimal control problems. See Figure 1 for an illustration of these correspondences. As such, our novel connection increases the interpretability of the training process of certain machine learning applications by showing that when we solve these learning problems, we actually solve a multi-time HJ PDE and by extension, its corresponding optimal control problem. In this paper, we show that our novel connection allows us to leverage HJ PDE and optimal control theory to solve optimization problems arising in certain machine learning applications, and we reserve the reverse direction for future work.

We focus on the connection between the regularized linear regression problem and

^{*}Division of Applied Mathematics, Brown University, Providence, RI 02912, USA (paula_chen@brown.edu, zongren_zou@brown.edu, jerome_darbon@brown.edu, george_karniadakis@brown.edu).

[†]Department of Mathematics, UCLA, Los Angeles, CA 90025, USA (tingwei@math.ucla.edu).

[‡]Paula Chen, Tingwei Meng, and Zongren Zou contributed equally to this work.

[§]Corresponding author.

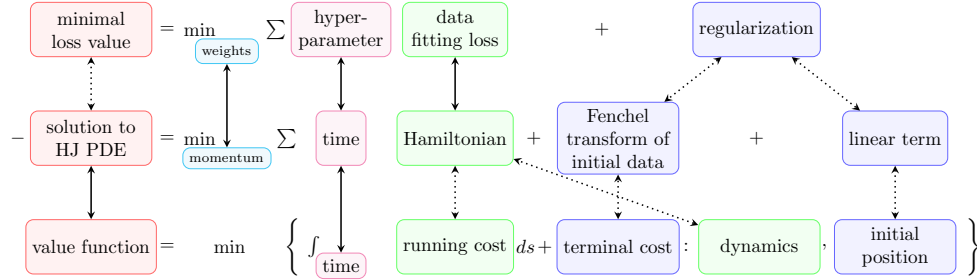


Fig. 1: (See Section 2) Illustration of a connection between a regularized learning problem (**top**), the multi-time Hopf formula (**middle**), and an optimal control problem (**bottom**). The colors indicate the associated quantities between each problem. For example, the optimal weights in the learning problem are equivalent to the momentum in the HJ PDE (cyan), and the hyper-parameters for the data fitting terms correspond to the time variables in the HJ PDE and the time horizon in the optimal control problem (magenta). This color scheme is reused in the subsequent illustrations of our connection. The solid-line arrows denote direct equivalences. The dotted arrows represent additional mathematical relations.

the Linear Quadratic Regulator (LQR) (Section 3). We use this case to gain a deeper understanding of our novel connection and illustrate its potential benefits. Linear regression consists of learning a linear prediction model and is one of the fundamental learning problems in supervised machine learning [30, 24, 35]. LQR [32] is a well-studied optimal control problem with certain quadratic running and terminal costs and linear dynamics and is typically solved using the Riccati ordinary differential equations (ODEs) [23, 6, 25]. Through our novel connection, we establish that solving certain regularized linear regression problems is equivalent to solving certain LQR problems. As a result, we can leverage standard LQR solvers to design new training approaches for machine learning. In particular, we develop new methodology for solving certain regularized linear regression problems by adapting solvers for the Riccati ODEs to these new settings (Section 4).

To highlight the versatility and possible computational advantages of our new Riccati-based approach, we apply our methodology to several test problems in machine learning (Section 5). In the first example, we consider a function approximation problem to demonstrate the computational and memory advantages of our Riccati-based approach in the context of continual learning [26, 19, 33]. Specifically, we show that our Riccati-based approach naturally enables us to continually adapt the learned model to new data without having to store or retrain on the previous data (which is especially significant given the rise of big data), while also avoiding catastrophic forgetting [19, 26]. In the second example, we demonstrate how our Riccati-based approach can be used to perform post-training calibrations. In particular, our approach gives us the flexibility to add or remove data points and tune hyper-parameters to increase the accuracy of the learned model without having to retrain it entirely, which again provides computational and memory advantages over conventional learning methods. In the third example, we use our Riccati-based method to fit the last layer of a physics-informed neural network (PINN) [28] using transfer learning [36, 11]. In this application, we demonstrate that as we change the value of the hyper-parameters,

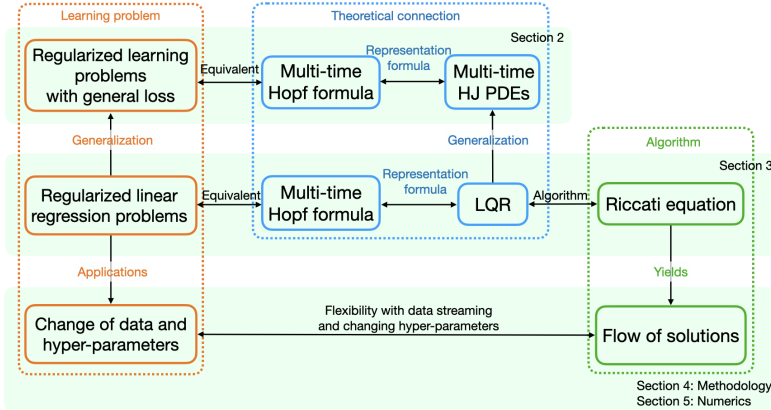


Fig. 2: Overview of the overall structure of this paper, the learning problems considered, our new theoretical connection, and our new Riccati-based algorithm. We show the learning problem in the **left** (orange), the theoretical connection in the **middle** (blue), and the algorithm in the **right** (green). The **top** row contains the general connection between learning problems and HJ PDEs (see Section 2), the **middle** row contains the connection between the regularized linear regression problem and LQR (see Section 3), and the **bottom** row contains the connection between applications in machine learning and our Riccati-based algorithm (see Sections 4 and 5).

solving the associated Riccati ODEs not only provides the solution to the updated problem, but also a *continuum* of solutions along a 1D curve on the Pareto front of the data fitting losses and regularization. Finally, in the fourth example, we highlight the versatility of our Riccati-based approach by showing how it can be combined with existing optimization methods (e.g., the primal-dual hybrid gradient (PDHG) algorithm [4]) to perform sparse dynamics identification [2].

The main contributions of this work are the development of a new theoretical connection between learning problems and the Hopf formula and a new Riccati-based approach for solving regularized linear regression problems. While we demonstrate promising results, the work presented here has some limitations. For example, while we establish our novel theoretical connection between more general learning problems, multi-time HJ PDEs, and optimal control problems, we have yet to fully explore non-linear learning models, general convex Hamiltonians, or non-linear control dynamics. Additionally, as discussed previously, we have also not yet investigated what possible advantages our novel connection provides for solving HJ PDEs and optimal control problems. In particular, many efficient solvers for high-dimensional problems in machine learning exist [20, 13]; it would be desirable to be able to leverage our connection to reuse this machinery for HJ PDEs and optimal control. Thus, our novel connection presents many exciting opportunities. We discuss some other possible future directions in Section 6. The overall structure of this paper is illustrated in Figure 2.

2. Generalized Hopf formula. In this section, we provide some mathematical background on the single- and multi-time Hopf formulas. Specifically, we review the well-known connections between the Hopf formula, the solution to the HJ PDEs, and the solution to the corresponding optimal control problems. We then present a novel theoretical connection between the Hopf formula and certain learning problems.

Through this connection, we establish that when we solve certain learning problems, we are actually evaluating the solution to certain HJ PDEs and their corresponding optimal control problems, and vice versa.

2.1. Introduction to the Hopf formula. The single-time HJ PDE is

$$(2.1) \quad \begin{cases} \frac{\partial S(\mathbf{x}, t)}{\partial t} + H(\nabla_{\mathbf{x}} S(\mathbf{x}, t)) = 0 & \mathbf{x} \in \mathbb{R}^n, t > 0, \\ S(\mathbf{x}, 0) = J(\mathbf{x}) & \mathbf{x} \in \mathbb{R}^n, \end{cases}$$

where $H : \mathbb{R}^n \rightarrow \mathbb{R}$ is the Hamiltonian and $J : \mathbb{R}^n \rightarrow \mathbb{R}$ is the initial condition. Assume that H and J are convex. Then, the viscosity solution to the single-time HJ PDE (2.1) is given by the Hopf formula [16]:

$$(2.2) \quad S(\mathbf{x}, t) = \sup_{\mathbf{p} \in \mathbb{R}^n} \{ \langle \mathbf{x}, \mathbf{p} \rangle - tH(\mathbf{p}) - J^*(\mathbf{p}) \} = - \inf_{\mathbf{p} \in \mathbb{R}^n} \{ tH(\mathbf{p}) + J^*(\mathbf{p}) - \langle \mathbf{x}, \mathbf{p} \rangle \},$$

where f^* denotes the Fenchel-Legendre transform of the function f ; i.e., $f^*(p) = \sup_{x \in \mathbb{R}^n} \{ \langle x, p \rangle - f(x) \}$.

The Hopf formula (2.2) also solves the following optimal control problem:

$$(2.3) \quad \min_{\mathbf{x}(\cdot)} \left\{ \int_0^t L(\mathbf{u}(s)) ds + J(\mathbf{x}(t)) : \dot{\mathbf{x}}(s) = f(\mathbf{u}(s)) \forall s \in (0, t], \mathbf{x}(0) = \mathbf{x} \right\},$$

where the running cost L and the source term f of the dynamics are related to the Hamiltonian H by $H(\mathbf{p}) = \sup_{\mathbf{u} \in \mathbb{R}^n} \{ \langle -f(\mathbf{u}), \mathbf{p} \rangle - L(\mathbf{u}) \}$ and, in this context, we interpret J to be the terminal cost.

A natural generalization of this formulation to the multi-time case is as follows. Let H_1, \dots, H_N be convex Hamiltonians, such that $\text{dom } H_i = \mathbb{R}^n$ for all $i = 1, \dots, N$, and let J be a convex initial condition. Then, the multi-time HJ PDE is given by

$$(2.4) \quad \begin{cases} \frac{\partial S(\mathbf{x}, t)}{\partial t_i} + H_i(\nabla_{\mathbf{x}} S(\mathbf{x}, t)) = 0 \text{ for } i \in \{1, \dots, N\} & \mathbf{x} \in \mathbb{R}^n, t_1, \dots, t_N > 0, \\ S(\mathbf{x}, 0, \dots, 0) = J(\mathbf{x}) & \mathbf{x} \in \mathbb{R}^n, \end{cases}$$

and the solution to the multi-time HJ PDE (2.4) can be represented by the following generalized (multi-time) Hopf formula [22]:

$$(2.5) \quad \begin{aligned} S(\mathbf{x}, t_1, \dots, t_N) &= \sup_{\mathbf{p} \in \mathbb{R}^n} \left\{ \langle \mathbf{x}, \mathbf{p} \rangle - \sum_{i=1}^N t_i H_i(\mathbf{p}) - J^*(\mathbf{p}) \right\} \\ &= - \inf_{\mathbf{p} \in \mathbb{R}^n} \left\{ \sum_{i=1}^N t_i H_i(\mathbf{p}) + J^*(\mathbf{p}) - \langle \mathbf{x}, \mathbf{p} \rangle \right\}. \end{aligned}$$

Moreover, the generalized Hopf formula (2.5) also solves an optimal control problem in the form of (2.3) with terminal time $t = \sum_{j=1}^N t_j$ and where the running cost L and the source term f of the dynamics are defined piecewise by $L(s, \mathbf{u}) = L_i(\mathbf{u})$ and $f(s, \mathbf{u}) = f_i(\mathbf{u})$, respectively, for $s \in \left(\sum_{j=1}^{i-1} t_j, \sum_{j=1}^i t_j \right]$ and $i = 1, \dots, N$. The piecewise running costs L_i and piecewise source terms f_i of the dynamics are related to the Hamiltonians H_i by $H_i(\mathbf{p}) = \sup_{\mathbf{u} \in \mathbb{R}^n} \{ \langle -f_i(\mathbf{u}), \mathbf{p} \rangle - L_i(\mathbf{u}) \}$.

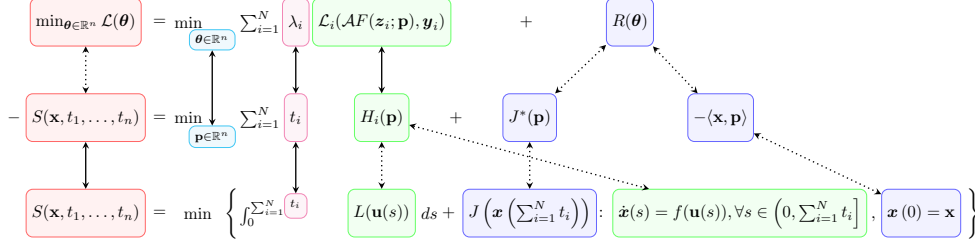


Fig. 3: (See Section 2) Mathematical formulation describing the connection between a regularized learning problem (**top**), the multi-time Hopf formula (**middle**), and an optimal control problem (**bottom**). The content of this illustration matches that of Figure 1 by replacing each term in Figure 1 with its corresponding mathematical expression. The colors indicate the associated quantities between each problem. The solid-line arrows denote direct equivalences. The dotted arrows represent additional mathematical relations.

2.2. Connection between the Hopf formula and learning problems.

In this section, we connect the Hopf formulas (2.2) and (2.5) with certain learning problems. Consider a learning problem with data points $\{(\mathbf{z}_i, \mathbf{y}_i)\}_{i=1}^N \subset \mathbb{R}^m \times \mathbb{R}^M$. The goal of the learning problem is to find a function $F(\mathbf{z}; \boldsymbol{\theta})$ with input $\mathbf{z} \in \mathbb{R}^m$ and unknown parameter $\boldsymbol{\theta} \in \mathbb{R}^n$, such that $\mathcal{A}F(\mathbf{z}_i; \boldsymbol{\theta})$ approximately equals \mathbf{y}_i at every \mathbf{z}_i . Here \mathcal{A} is an operator acting on the function F . For instance, \mathcal{A} could be the identity operator (as in the regression problem [35]) or a differential operator (as in PINNs [28]). Then, the learning problem is given by the following optimization problem:

$$(2.6) \quad \min_{\boldsymbol{\theta} \in \mathbb{R}^n} \sum_{i=1}^N \lambda_i \mathcal{L}_i(\mathcal{A}F(\mathbf{z}_i; \boldsymbol{\theta}), \mathbf{y}_i) + R(\boldsymbol{\theta}).$$

The above loss function consists of two parts: each of $\mathcal{L}_i(\mathcal{A}F(\mathbf{z}_i; \boldsymbol{\theta}), \mathbf{y}_i)$ is a data fitting term at $(\mathbf{z}_i, \mathbf{y}_i)$ (where $\mathcal{L}_i(\mathbf{a}, \mathbf{b})$ is a function measuring the discrepancy between \mathbf{a} and \mathbf{b}) and R is a regularization term. In this paper, we assume the function $\boldsymbol{\theta} \mapsto \mathcal{L}_i(\mathcal{A}F(\mathbf{z}_i; \boldsymbol{\theta}), \mathbf{y}_i)$ is convex for all $i = 1, \dots, N$.

Then, the connection between the learning problem (2.6), the Hopf formulas (2.2) and (2.5), and the optimal control problem (2.3) is illustrated in Figure 3. Specifically, if there is only one data point ($N = 1$), the learning problem (2.6) is related to the single-time Hopf formula (2.2) by setting $H(\mathbf{p}) = \mathcal{L}_1(\mathcal{A}F(\mathbf{z}_1; \mathbf{p}), \mathbf{y}_1)$, $t = \lambda_1$, and $R(\mathbf{p}) = J^*(\mathbf{p}) - \langle \mathbf{x}, \mathbf{p} \rangle$. Hence, when we solve these single-point learning problems, we simultaneously evaluate the solution to the HJ PDE (2.1) at the point (\mathbf{x}, t) , or equivalently, we solve the corresponding optimal control problem (2.3). Conversely, when we solve the HJ PDE (2.1), the spatial gradient $\nabla_{\mathbf{x}} S(\mathbf{x}, t)$ of the solution gives the minimizer $\boldsymbol{\theta}^*$ to the single-point learning problem (2.6).

If there are $N > 1$ data points, then the learning problem (2.6) is related to the multi-time Hopf formula (2.5) by setting $H_i(\mathbf{p}) = \mathcal{L}_i(\mathcal{A}F(\mathbf{z}_i; \mathbf{p}), \mathbf{y}_i)$, $t_i = \lambda_i$, and $R(\mathbf{p}) = J^*(\mathbf{p}) - \langle \mathbf{x}, \mathbf{p} \rangle$. Hence, solving these multi-point learning problems is equivalent to evaluating the solution to the HJ PDE (2.5) at the point $(\mathbf{x}, t_1, \dots, t_N)$, which is also equivalent to solving the corresponding optimal control problem (2.3) with terminal time $t = \sum_{j=1}^N t_j$ and piecewise running costs L_i and dynamics f_i related via $H_i(\mathbf{p}) = \sup_{\mathbf{u} \in \mathbb{R}^n} \{-f_i(\mathbf{u}, \mathbf{p}) - L_i(\mathbf{u})\}$. Similarly to the single-time case,

when we solve the multi-time HJ PDE (2.4), the spatial gradient $\nabla_{\mathbf{x}}S(\mathbf{x}, t_1, \dots, t_N)$ of the solution gives the minimizer $\boldsymbol{\theta}^*$ to the multi-point learning problem (2.6).

3. Linear Quadratic Regulator. In this section, we develop our theoretical connection from Section 2.2 in the specific case where the optimal control problem (2.3) corresponds to the LQR problem [32]. We show that solving certain LQR problems is equivalent to solving learning problems with linear models, quadratic data fitting losses, and quadratic regularization (i.e., an ℓ_2 -regularized linear regression problem). Although broader classes of learning problems are of interest, we restrict to linear regression problems as a starting point for demonstrating the potential of our theoretical connection. Specifically, we leverage our novel theoretical connection to show how established techniques for solving certain HJ PDEs (e.g., the Riccati ODEs [23]) can be reused to solve this class of learning problems.

3.1. Introduction to the Linear Quadratic Regulator and Riccati equation. The finite-horizon, continuous-time LQR is given by

$$(3.1) \quad S(\mathbf{x}, t) = \min \left\{ \int_0^t \left(\frac{1}{2} \mathbf{x}(s)^T \mathcal{Q} \mathbf{x}(s) + \frac{1}{2} \mathbf{u}(s)^T \mathcal{R} \mathbf{u}(s) + \mathbf{x}(s)^T \mathcal{N} \mathbf{u}(s) \right) ds + \frac{1}{2} \mathbf{x}(t)^T \mathcal{Q}_f \mathbf{x}(t) : \dot{\mathbf{x}}(s) = A \mathbf{x}(s) + B \mathbf{u}(s) \forall s \in (0, t], \mathbf{x}(0) = \mathbf{x} \right\},$$

where $\mathcal{Q}, \mathcal{Q}_f \in \mathbb{R}^{n \times n}$ and $\mathcal{R} \in \mathbb{R}^{m \times m}$ are symmetric positive definite, $\mathcal{N} \in \mathbb{R}^{n \times m}$, $A \in \mathbb{R}^{n \times n}$, and $B \in \mathbb{R}^{n \times m}$. The corresponding HJ PDE is

$$(3.2) \quad \begin{cases} \frac{\partial S(\mathbf{x}, t)}{\partial t} + H(\mathbf{x}, \nabla_{\mathbf{x}} S(\mathbf{x}, t)) = 0 & \mathbf{x} \in \mathbb{R}^n, t > 0 \\ S(\mathbf{x}, 0) = J(\mathbf{x}) & \mathbf{x} \in \mathbb{R}^n, \end{cases}$$

where the initial data of the HJ PDE is given by the terminal cost $J(\mathbf{x}) := \frac{1}{2} \mathbf{x}^T \mathcal{Q}_f \mathbf{x}$ of the optimal control problem and the Hamiltonian H is defined by

$$(3.3) \quad \begin{aligned} H(\mathbf{x}, \mathbf{p}) &= \sup_{\mathbf{u} \in \mathbb{R}^m} \langle -f(\mathbf{x}, \mathbf{u}), \mathbf{p} \rangle - L(\mathbf{x}, \mathbf{u}) \\ &= -\langle A \mathbf{x}, \mathbf{p} \rangle - \frac{1}{2} \langle \mathbf{x}, \mathcal{Q} \mathbf{x} \rangle + \frac{1}{2} \langle B^T \mathbf{p} + \mathcal{N}^T \mathbf{x}, \mathcal{R}^{-1} (B^T \mathbf{p} + \mathcal{N}^T \mathbf{x}) \rangle, \end{aligned}$$

where $f(\mathbf{x}, \mathbf{u}) = A \mathbf{x} + B \mathbf{u}$ is the source term of the dynamics and $L(\mathbf{x}, \mathbf{u}) = \frac{1}{2} \mathbf{x}^T \mathcal{Q} \mathbf{x} + \frac{1}{2} \mathbf{u}^T \mathcal{R} \mathbf{u} + \mathbf{x}^T \mathcal{N} \mathbf{u}$ is the running cost. Note that because of the spatial dependence in the Hamiltonian H , the Hopf formula cannot be applied directly to the above LQR problem without additional assumptions. In Sections 3.2 and 3.3, we discuss some assumptions under which H is independent of the spatial variable \mathbf{x} and the corresponding learning problems that can be solved via our connection through the Hopf formula (see, for example, Figure 4).

It is well-known that this LQR problem can be solved using the Riccati equation as follows [23]. Define $C_{pp} = B \mathcal{R}^{-1} B^T$, $C_{xx} = -\mathcal{N} \mathcal{R}^{-1} \mathcal{N}^T + \mathcal{Q}$, and $C_{xp} = A - B \mathcal{R}^{-1} \mathcal{N}^T$. Then, the solution is also given by $S(\mathbf{x}, t) = \frac{1}{2} \mathbf{x}^T P(t) \mathbf{x}$, where the function $P : [0, \infty) \rightarrow \mathbb{R}^{n \times n}$ takes values in the space of symmetric positive definite matrices and solves the following Riccati equation:

$$(3.4) \quad \begin{cases} \dot{P}(t) = -P(t)^T C_{pp} P(t) + P(t)^T C_{xp} + C_{xp}^T P(t) + C_{xx} & t \in (0, +\infty), \\ P(0) = \mathcal{Q}_f. \end{cases}$$

When H does not depend on \mathbf{x} , we can use our connection to modify the corresponding LQR problem to consider different HJ PDEs and, hence, to accommodate different learning problems. For example, adding lower order terms in the running cost L and/or the source term f of the dynamics corresponds to adding lower order terms in the Hamiltonian of the HJ PDE or, equivalently, in the data fitting term of the learning problem. Similarly, adding lower order terms in the terminal cost J corresponds to adding lower order terms in the initial condition of the HJ PDE or, equivalently, in the regularization term of the learning problem.

3.2. Connection to single-point regularized linear regression problems.

In this section, we establish a relation between the linear regression problem with only one data point and the LQR problem (3.1) with $A = \mathcal{Q} = 0$ and $\mathcal{N} = 0$. Note that, to do this, we also add in some lower order terms to the original LQR problem (3.1). In this case, the LQR problem becomes

$$(3.5) \quad S(\mathbf{x}, t) = \min \left\{ \int_0^t \left(\frac{1}{2} \mathbf{u}(s)^T \mathcal{R} \mathbf{u}(s) - \mathbf{a}^T \mathbf{u}(s) \right) ds + \frac{1}{2} \mathbf{x}(t)^T \mathcal{Q}_f \mathbf{x}(t) + \mathbf{b}^T \mathbf{x}(t) : \dot{\mathbf{x}}(s) = B \mathbf{u}(s) \forall s \in (0, t], \mathbf{x}(0) = \mathbf{x} \right\},$$

and the corresponding HJ PDE is given by (3.2), where $J(\mathbf{x}) = \frac{1}{2} \mathbf{x}^T \mathcal{Q}_f \mathbf{x} + \mathbf{b}^T \mathbf{x}$ is the initial data/terminal cost whose Fenchel transform is given by

$$J^*(\mathbf{p}) = \sup_{\mathbf{x} \in \mathbb{R}^n} \langle \mathbf{x}, \mathbf{p} \rangle - J(\mathbf{x}) = \frac{1}{2} \left\| \mathcal{Q}_f^{-1/2} (\mathbf{p} - \mathbf{b}) \right\|_2^2$$

and the Hamiltonian H is given by

$$H(\mathbf{p}) = \sup_{\mathbf{u} \in \mathbb{R}^n} \langle -B \mathbf{u}, \mathbf{p} \rangle - \frac{1}{2} \mathbf{u}^T \mathcal{R} \mathbf{u} + \mathbf{a}^T \mathbf{u} = \frac{1}{2} \left\| \mathcal{R}^{-1/2} (B^T \mathbf{p} - \mathbf{a}) \right\|_2^2,$$

where $f(\mathbf{u}) = B \mathbf{u}$ is the source term of the dynamics and $L(\mathbf{u}) = \frac{1}{2} \mathbf{u}^T \mathcal{R} \mathbf{u}$ is the running cost. Then, using the single-time Hopf formula (2.2), we have that the solution to the HJ PDE is given by

$$(3.6) \quad S(\mathbf{x}, t) = \sup_{\mathbf{p} \in \mathbb{R}^n} \left\{ \langle \mathbf{x}, \mathbf{p} \rangle - \frac{t}{2} \left\| \mathcal{R}^{-1/2} (B^T \mathbf{p} - \mathbf{a}) \right\|_2^2 - \frac{1}{2} \left\| \mathcal{Q}_f^{-1/2} (\mathbf{p} - \mathbf{b}) \right\|_2^2 \right\}.$$

In this case, we can compute the maximizer in the above Hopf formula explicitly, which can be done numerically using the method of least squares. Alternatively, this LQR problem can also be solved via the Riccati ODEs, which are given by

$$(3.7) \quad \dot{P}(t) = -P(t)^T B \mathcal{R}^{-1} B^T P(t), \quad \dot{\mathbf{q}}(t) = -P(t)^T B \mathcal{R}^{-1} (B^T \mathbf{q}(t) - \mathbf{a}),$$

$$\dot{r}(t) = -\frac{1}{2} \left\| \mathcal{R}^{-1/2} (B^T \mathbf{q}(t) - \mathbf{a}) \right\|_2^2,$$

with initial conditions $P(0) = \mathcal{Q}_f$, $\mathbf{q}(0) = \mathbf{b}$, and $r(0) = 0$.

The above Hopf formula (3.6) is related to the learning problem (2.6) with quadratic data fidelity term and quadratic regularization. Specifically, let $t = \lambda$ and

$\mathbf{p} = \boldsymbol{\theta}$. Then, solving the above maximization problem (3.6) is equivalent to minimizing the following loss function with respect to $\boldsymbol{\theta} = [\theta_1, \dots, \theta_n]^T$:

$$(3.8) \quad \mathcal{L}(\boldsymbol{\theta}) = \frac{\lambda}{2} \left\| \mathcal{R}^{-1/2}(B^T \boldsymbol{\theta} - \mathbf{a}) \right\|_2^2 + \frac{1}{2} \left\| \mathcal{Q}_f^{-1/2}(\boldsymbol{\theta} - (\mathbf{b} + \mathcal{Q}_f \mathbf{x})) \right\|_2^2.$$

This loss function corresponds to a one-point linear regression problem, where the regularization term is given by $\frac{1}{2} \left\| \mathcal{Q}_f^{-1/2}(\boldsymbol{\theta} - (\mathbf{b} + \mathcal{Q}_f \mathbf{x})) \right\|_2^2$ and the data fitting term is given by $\frac{\lambda}{2} \left\| \mathcal{R}^{-1/2}(B^T \boldsymbol{\theta} - \mathbf{a}) \right\|_2^2$; i.e., set $N = 1$ in Figure 4. The minimizer $\boldsymbol{\theta}^*$ of \mathcal{L} is related to the solution of the Riccati equation via

$$(3.9) \quad \boldsymbol{\theta}^*(= \mathbf{p}^*) = \nabla_{\mathbf{x}} S(\mathbf{x}, \lambda) = P(\lambda) \mathbf{x} + \mathbf{q}(\lambda),$$

where \mathbf{p}^* is the minimizer in the Hopf formula (3.6). Note that if we only need to recover the minimizer $\boldsymbol{\theta}^*$, then we only need to solve two ODEs (i.e., the ODEs for P, \mathbf{q}) since (3.9) does not depend on r .

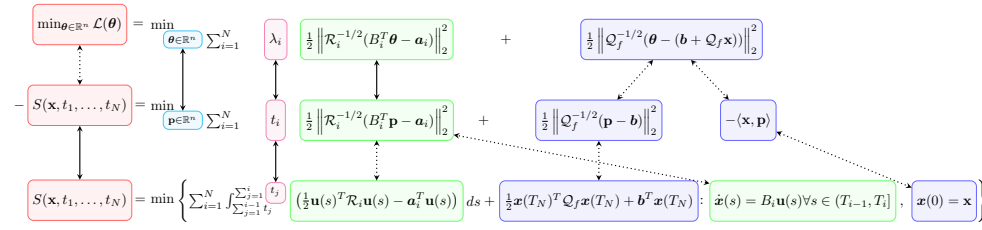


Fig. 4: (See Section 3) Mathematical formulation describing the connection between a regularized linear regression problem (**top**), the multi-time Hopf formula (**middle**), and a piecewise LQR problem with $A = \mathcal{Q} = 0$ and $\mathcal{N} = 0$ on each piece (**bottom**). Note that $T_i = \sum_{j=1}^i t_j$. The content of this illustration is a special case of the connection in Figure 3 using quadratic data fitting losses and quadratic regularization. The colors indicate the associated quantities between each problem. The solid-line arrows denote direct equivalences. The dotted arrows represent additional mathematical relations.

3.3. Connection to multi-point regularized linear regression problems.

If the running cost is piecewise quadratic with $\mathcal{Q} = 0, \mathcal{N} = 0$ on each piece and the dynamics are piecewise linear with $A = 0$ on each piece, then we get a more general piecewise LQR problem in the form of (2.3) with piecewise running costs $L_i(\mathbf{u}) = \frac{1}{2} \mathbf{u}^T \mathcal{R}_i \mathbf{u} - \mathbf{a}_i^T \mathbf{u}$, piecewise dynamics $f_i(\mathbf{u}) = B_i \mathbf{u}$, terminal cost $J(\mathbf{x}) = \frac{1}{2} \mathbf{x}^T \mathcal{Q}_f \mathbf{x} + \mathbf{b}^T \mathbf{x}$, and terminal time $t = \sum_{j=1}^N t_j$. Recall that this optimal control problem corresponds to the multi-time HJ PDE (2.4) with Hamiltonians $H_i(\mathbf{p}) = \sup_{\mathbf{u} \in \mathbb{R}^n} \{ \langle -f_i(\mathbf{u}), \mathbf{p} \rangle - L_i(\mathbf{u}) \}$ and initial data J . Then, the solution to this LQR problem and corresponding HJ PDE is given by the following multi-time Hopf formula: (3.10)

$$(3.10) \quad S(\mathbf{x}, t_1, \dots, t_N) = \sup_{\mathbf{p} \in \mathbb{R}^n} \left\{ \langle \mathbf{x}, \mathbf{p} \rangle - \sum_{i=1}^N \frac{t_i}{2} \left\| \mathcal{R}_i^{-1/2}(B_i^T \mathbf{p} - \mathbf{a}_i) \right\|_2^2 - \frac{1}{2} \left\| \mathcal{Q}_f^{-1/2}(\mathbf{p} - \mathbf{b}) \right\|_2^2 \right\}.$$

Define T_m to be

$$(3.11) \quad T_m = \sum_{j=1}^m t_j.$$

Then, the multi-time HJ PDE and piecewise LQR problem can also be solved using the following Riccati equation: $S(\mathbf{x}, t_1, \dots, t_N) = \frac{1}{2} \mathbf{x}^T P(T_N) \mathbf{x} + \mathbf{q}(T_N)^T \mathbf{x} + r(T_N)$, where the function $P : [0, \infty) \rightarrow \mathbb{R}^{n \times n}$ takes values in the space of symmetric positive definite matrices and solves the following piecewise Riccati equation:

$$(3.12) \quad \begin{cases} \dot{P}(s) = -P(s)^T B_i \mathcal{R}_i^{-1} B_i^T P(s) & s \in (T_{i-1}, T_i) \\ P(0) = \mathcal{Q}_f, \end{cases}$$

the function $\mathbf{q} : [0, \infty) \rightarrow \mathbb{R}^n$ solves the following piecewise linear ODE:

$$(3.13) \quad \begin{cases} \dot{\mathbf{q}}(s) = -P(s)^T B_i \mathcal{R}_i^{-1} (B_i^T \mathbf{q}(s) - \mathbf{a}_i) & s \in (T_{i-1}, T_i), \\ \mathbf{q}(0) = -\mathbf{b}, \end{cases}$$

and the function $r : [0, \infty) \rightarrow \mathbb{R}$ solves the following piecewise ODE:

$$(3.14) \quad \begin{cases} \dot{r}(s) = -\frac{1}{2} \left\| \mathcal{R}_i^{-1/2} (B_i^T \mathbf{q}(s) - \mathbf{a}_i) \right\|_2^2 & s \in (T_{i-1}, T_i), \\ r(0) = 0. \end{cases}$$

The above multi-time Hopf formula (3.10) can also be regarded as a linear regression problem with multiple data points, as illustrated in Figure 4. Let $\frac{1}{2} \left\| \mathcal{Q}_f^{-1/2} (\mathbf{p} - \mathbf{b}) \right\|_2^2$ be the regularization term and $\frac{t_i}{2} \left\| \mathcal{R}_i^{-1/2} (B_i^T \mathbf{p} - \mathbf{a}_i) \right\|_2^2$ be the data fitting term at the i -th data point. Then, the multi-time LQR problem (3.10) is equivalent to the learning problem $\min_{\boldsymbol{\theta}} \mathcal{L}(\boldsymbol{\theta})$, where the loss function $\mathcal{L} : \mathbb{R}^n \rightarrow \mathbb{R}$ is given by

$$(3.15) \quad \mathcal{L}(\boldsymbol{\theta}) = \sum_{i=1}^N \frac{\lambda_i}{2} \left\| \mathcal{R}_i^{-1/2} (B_i^T \boldsymbol{\theta} - \mathbf{a}_i) \right\|_2^2 + \frac{1}{2} \left\| \mathcal{Q}_f^{-1/2} (\boldsymbol{\theta} - (\mathbf{b} + \mathcal{Q}_f \mathbf{x})) \right\|_2^2.$$

In Section 4.1, we discuss a specific example of the learning problem (3.15), which is more readily recognizable as the standard linear regression problem. The minimizer $\boldsymbol{\theta}^*$ of the learning problem (3.15) (and \mathbf{p}^* of the Hopf formula (3.10)) is given by

$$(3.16) \quad \boldsymbol{\theta}^* (= \mathbf{p}^*) = \nabla_{\mathbf{x}} S(\mathbf{x}, t_1, \dots, t_N) = P(T_N) \mathbf{x} + \mathbf{q}(T_N).$$

4. Methodology. In the previous section, we established a novel theoretical connection between certain multi-time HJ PDEs, LQR problems, and regularized linear regression problems. In this section, we leverage this theoretical connection to design novel algorithms for solving various learning problems. The connection between the learning problem of interest, the Hopf formula, and the corresponding optimal control problem is summarized in Figure 5 and Table 1.

4.1. Solving the regularized linear regression problem using Riccati ODEs. A linear regression problem with quadratic data fitting loss and quadratic regularization is formulated as follows. The goal of this learning problem is to fit N data points $(\mathbf{z}_i, \mathbf{y}_i) \in \mathbb{R}^m \times \mathbb{R}^M$ with the linear prediction model $\Phi_i \boldsymbol{\theta} \approx \mathbf{y}_i$, where

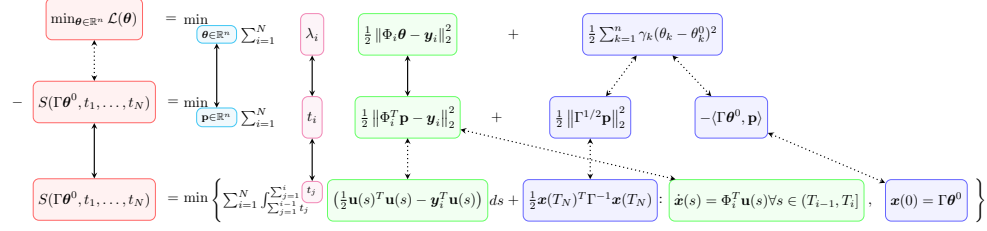


Fig. 5: (See Section 4) Mathematical formulation describing the connection between our model linear regression problem with quadratic regularization (**top**), the multi-time Hopf formula (**middle**), and a piecewise LQR problem (**bottom**). Note that $T_i = \sum_{j=1}^i t_j$. The content of this illustration is a special case of the connection in Figure 4 using $\mathcal{R}_i = I$, $B_i = \Phi_i^T$, $\mathbf{a}_i = \mathbf{y}_i$, $\mathcal{Q}_f = \Gamma^{-1}$, $\mathbf{b} = 0$, and $\mathbf{x} = \Gamma \theta^0$. We use this connection to develop our Riccati-based methodology (Section 4) and perform our numerical examples (Section 5). The colors indicate the associated quantities between each problem. The solid-line arrows denote direct equivalences. The dotted arrows represent additional mathematical relations.

Terms in the loss function (4.1)	Terms in the Hopf formula	Terms in the optimal control problem	Learning problems
Φ_i, \mathbf{y}_i	Hamiltonian	Running cost, dynamics	Continual learning (Section 5.1); Post-training calibration (Section 5.2)
λ_i	Time	Time	Post-training calibration (Section 5.2)
γ_k	Hamiltonian; Initial condition	Running cost, dynamics; Terminal cost	Hyper-parameter tuning, flow along the Pareto front (Section 5.3)
θ_k^0	Spatial variable	Initial position	Generalized regularization functions (Section 5.4)

Table 1: Summary of the learning problems and corresponding numerical examples presented in this work. Each row summarizes which terms in the loss function (4.1), the Hopf formula, and the optimal control problem must be changed to match the context of various learning problems.

$\Phi_i = [\phi_1(\mathbf{z}_i), \dots, \phi_n(\mathbf{z}_i)] \in \mathbb{R}^{M \times n}$ is the matrix whose columns are the basis functions $\phi_j : \mathbb{R}^m \rightarrow \mathbb{R}^M$, $j = 1, \dots, n$ evaluated at \mathbf{z}_i and $\theta = [\theta_1, \dots, \theta_n]^T \in \mathbb{R}^n$ are unknown trainable coefficients. We learn $\theta \in \mathbb{R}^n$ by minimizing the following loss function:

$$(4.1) \quad \mathcal{L}(\theta) = \frac{1}{2} \sum_{i=1}^N \lambda_i \|\Phi_i \theta - \mathbf{y}_i\|_2^2 + \frac{1}{2} \sum_{k=1}^n \gamma_k (\theta_k - \theta_k^0)^2,$$

where $\lambda_i \geq 0, i = 1, \dots, N$ are tunable hyper-parameters for the data fitting losses, $\gamma_k > 0, k = 1, \dots, n$ are tunable hyper-parameters for the regularization terms, and $\theta_k^0 \in \mathbb{R}$ is a prior on the unknown coefficients that biases θ_k to be close to θ_k^0 . Note that the above loss function (4.1) is strictly convex, and hence it has a unique global minimizer. Since this loss function is quadratic in θ , it can be minimized exactly using the method of least squares. However, we explore a different approach for minimizing (4.1), which, in certain learning contexts, yields computational advantages over conventional approaches like the method of least squares.

Note that this learning problem is in the form of (3.15); i.e., set $\mathcal{R}_i = I_{M \times M}$, $B_i = \Phi_i^T$, $\mathbf{a}_i = \mathbf{y}_i$, $\mathcal{Q}_f = \Gamma^{-1}$, where $\Gamma \in \mathbb{R}^{n \times n}$ is the diagonal matrix whose i -th entry is γ_i , $\mathbf{b} = 0$, and $\mathbf{x} = \Gamma \theta^0$. Then, this learning problem is related to an LQR

problem, and we summarize this connection in Figure 5. Thus, this learning problem can alternatively be solved via the following Riccati ODEs:

$$(4.2) \quad \begin{cases} \dot{P}(t) = -P(t)^T \Phi_i^T \Phi_i P(t) & t \in (T_{i-1}, T_i), \\ \dot{\mathbf{q}}(t) = -P(t)^T \Phi_i^T (\Phi_i \mathbf{q}(t) - \mathbf{y}_i) & t \in (T_{i-1}, T_i), \end{cases}$$

with initial condition $P(0) = \Gamma^{-1}$, $\mathbf{q}(0) = 0$. Note that here we disregard the ODE for r since, for the learning problem, we are only concerned with the value of the minimizer $\boldsymbol{\theta}^*$, which only requires the values of P, \mathbf{q} (e.g., see (3.9), (3.16)), whereas recovering the minimal objective value $\mathcal{L}(\boldsymbol{\theta}^*)$ (which is generally not needed in the context of learning) would require all three values P, \mathbf{q}, r . There are many numerical methods for solving the Riccati ODEs (4.2) in the literature. In this paper, we use the 4th-order Runge-Kutta method (RK4) [3].

At first glance, solving this linear regression problem via the Riccati ODEs (4.2) may seem unnecessary given the existence of other well-established methods for minimizing (4.1) (e.g., the method of least squares). However, note that (4.2) is actually a sequence of Riccati ODEs. Thus, using our theoretical connection (and hence, these sequential Riccati ODEs to minimize (4.1)) means that we have the flexibility to handle sequential changes to the learning problem. In the remainder of Section 4, we identify several applications in learning (summarized in Table 1), for which this Riccati-based approach yields computational advantages over traditional learning methods (especially when the number of data points N is large), and we describe how standard Riccati solvers can be adapted for these contexts.

4.2. Adding or removing data. Since our theoretical connection gives us access to the Riccati ODEs (4.2), which are solved sequentially, we have the flexibility to handle sequential changes to the learning problem (4.1). In this section, we focus on the sequential addition or removal of data. Some related machine learning examples are provided in Sections 5.1 and 5.2.

First, we discuss the addition of one data point; i.e., we increase the number of data points from N to $N + 1$. This case corresponds to updating our learned model as new data is collected, which is crucial for many practical machine learning applications. To add one data point, we adapt the Riccati ODEs (4.2) as follows. Adding the $(N + 1)$ -th data point corresponds to adding the term $\frac{1}{2} \lambda_{N+1} \|\Phi_{N+1} \boldsymbol{\theta} - \mathbf{y}_{N+1}\|_2^2$ in the loss function (4.1) or, equivalently, to adding the Hamiltonian $\frac{1}{2} \|\Phi_{N+1} \boldsymbol{\theta} - \mathbf{y}_{N+1}\|_2^2$ to the multi-time HJ PDE and the pieces $L_{N+1}(s, \mathbf{u}) = \frac{1}{2} \mathbf{u}^T \mathbf{u} - \mathbf{y}_{N+1}^T \mathbf{u}$ and $f(s, \mathbf{u}) = \Phi_{N+1}^T \mathbf{u}$, $s \in (T_N, T_{N+1})$ to the running cost and dynamics, respectively, of the corresponding piecewise LQR problem. Thus, minimizing this new loss function is equivalent to solving the following Riccati ODE:

$$(4.3) \quad \begin{cases} \dot{\tilde{P}}(t) = -\tilde{P}(t)^T \Phi_j^T \Phi_j \tilde{P}(t) & t > 0, \\ \dot{\tilde{\mathbf{q}}}(t) = -\tilde{P}(t)^T \Phi_j^T (\Phi_j \tilde{\mathbf{q}}(t) - \mathbf{y}_j) & t > 0, \end{cases}$$

where the index $j = N + 1$ and with initial condition $\tilde{P}(0) = P(T_N)$ and $\tilde{\mathbf{q}}(0) = \mathbf{q}(T_N)$, where $P(T_N)$ and $\mathbf{q}(T_N)$ are obtained from solving the learning problem (4.1) with N data points. Then, the solution to the new learning problem with an additional point is given by

$$(4.4) \quad \tilde{\boldsymbol{\theta}}^* = \tilde{P} \Gamma \boldsymbol{\theta}^0 + \tilde{\mathbf{q}},$$

where $\tilde{P} = \tilde{P}(\lambda_{N+1})(= P(T_{N+1}))$ and $\tilde{\mathbf{q}} = \tilde{\mathbf{q}}(\lambda_{N+1})(= \mathbf{q}(T_{N+1}))$ are the solution to (4.3); i.e., we have evolved the solution of the new corresponding multi-time HJ

PDE in the time variable t_{N+1} from $S(\mathbf{x}, t_1, \dots, t_N, 0)$ to $S(\mathbf{x}, t_1, \dots, t_N, \lambda_{N+1})$. Using the same methodology described above, note that we can also interpret adding one data point as solving a one-point linear regression problem (3.8) and its corresponding single-piece LQR problem (3.5).

Removing one data point (i.e., decreasing the number of data points from N to $N - 1$) corresponds to calibrating our learned model by removing possible outliers and/or overly noisy data. To remove one data point, we reverse time and solve a terminal value Riccati ODE (A.1). The solution to the new learning problem is then given by (4.4), where \tilde{P} , $\tilde{\mathbf{q}}$ are given by the solution to the time-reversed Riccati ODEs. For more details and the mathematical derivation, see Appendix A.1.

Note that in both cases, the above approach only requires information about the data point to be added or removed and the results of the previous training. Thus, we can add and remove data without retraining on the entire dataset or requiring access to all of the previous data. In contrast, traditional approaches to minimizing (4.1) (e.g., the method of least squares) would require memory of all previous data and then retraining on the entire updated data set. Hence, our approach provides promising computational and memory savings over conventional methods.

4.3. Hyper-parameter tuning. In the loss function (4.1), we have three types of hyper-parameters: the weights λ_i of the data fitting terms, the weights γ_k of the regularization term, and the bias $\boldsymbol{\theta}^0$ on the trainable coefficients $\boldsymbol{\theta}$. In this section, we discuss how we adapt the Riccati ODEs to tune each of these hyper-parameters.

First, we discuss tuning the weights of the data fitting terms; e.g., as in post-training calibration and federated learning (Section 5.2). Consider changing the weight on the i -th data fitting term from λ_i to $\tilde{\lambda}_i$, which corresponds to changing the time $t_i = \lambda_i$ to $t_i = \tilde{\lambda}_i$ in the multi-time HJ PDE and corresponding piecewise LQR problem. Then, the methodology is similar to that in Section 4.1.

If $\tilde{\lambda}_i > \lambda_i$, then the solution to the learning problem with the new data fitting weight $\tilde{\lambda}_i$ is given by (4.4), where $\tilde{P} = \tilde{P}(\tilde{\lambda}_i - \lambda_i)$ and $\tilde{\mathbf{q}} = \tilde{\mathbf{q}}(\tilde{\lambda}_i - \lambda_i)$ are the solutions to the Riccati ODEs (4.3) with $j = i$, at time $(\tilde{\lambda}_i - \lambda_i)$, and with initial condition $\tilde{P}(0) = P(T_N)$ and $\tilde{\mathbf{q}}(0) = \mathbf{q}(T_N)$, where $P(T_N), \mathbf{q}(T_N)$ are obtained from solving the original learning problem (4.1) with the original value of λ_i . Similarly, if $\lambda_i > \tilde{\lambda}_i$, then the solution to the learning problem with the new data fitting weight $\tilde{\lambda}_i$ is given by (4.4), where $\tilde{P} = \tilde{P}(0)$ and $\tilde{\mathbf{q}} = \tilde{\mathbf{q}}(0)$ are the solutions to the time-reversed Riccati ODEs (A.1) with $j = i$, at time 0, and with terminal condition $\tilde{P}(\lambda_i - \tilde{\lambda}_i) = P(T_N)$ and $\tilde{\mathbf{q}}(\lambda_i - \tilde{\lambda}_i) = \mathbf{q}(T_N)$, where $P(T_N), \mathbf{q}(T_N)$ are obtained from solving the original learning problem (4.1) with the original value of λ_i .

Next, we discuss tuning the weights of the regularization terms; e.g., as in the hyper-parameter tuning example in Section 5.3. Note that in the original formulation of the Riccati ODEs (4.2), the regularization weights appear in the initial condition for P . Changing a hyper-parameter γ_k by changing this initial condition would require re-solving the entire sequence of Riccati ODEs and hence retraining on the entire dataset. However, since we have freedom in how we formulate the corresponding multi-time HJ PDE, we can avoid this retraining as follows. Note that here, instead of sequentially changing each regularization weight γ_k one-by-one, we can actually update all of the regularization weights at once.

We update the regularization weights in two steps. First, we update the weights whose values we increase by adding an additional Hamiltonian to the multi-time HJ PDE. This yields an initial value Riccati ODE (A.2). Second, we update the remaining weights by reinterpreting the problem as a terminal condition, single-time

HJ PDE. We then evolve this HJ PDE backward in time using a terminal condition Riccati ODE (A.3). Finally, the minimizer to the new learning problem resulting from changing all of the regularization weights is the given by the solutions to the time-reversed Riccati ODE (A.3) at time 0. For more details, see Appendix A.2.

Finally, we discuss tuning the bias $\boldsymbol{\theta}^0$ on the trainable coefficients $\boldsymbol{\theta}$; e.g., as in the generalized regularization example in Section 5.4. In the context of the learning problem, we interpret $\boldsymbol{\theta}^0$ as the center of a Gaussian prior on $\boldsymbol{\theta}$. Using our theoretical connection, changing $\boldsymbol{\theta}^0$ is also equivalent to evaluating the corresponding multi-time HJ PDE and piecewise LQR problem at a different point in space. Specifically, changing $\boldsymbol{\theta}^0$ to $\tilde{\boldsymbol{\theta}}^0$ means that instead of evaluating the multi-time HJ PDE and piecewise LQR problem at $\mathbf{x} = \Gamma\boldsymbol{\theta}^0$, we evaluate them at $\mathbf{x} = \Gamma\tilde{\boldsymbol{\theta}}^0$. Then, the solution to the learning problem with the new bias $\tilde{\boldsymbol{\theta}}^0$ is given by

$$(4.5) \quad P(T_N)\Gamma\tilde{\boldsymbol{\theta}}^0 + \mathbf{q}(T_N),$$

where $P(T_N)$ and $\mathbf{q}(T_N)$ are obtained from solving the original learning problem (4.1) with the original value of $\boldsymbol{\theta}^0$. In other words, shifting the bias involves neither retraining nor access to any of the data points nor solving Riccati ODEs. Instead, we only require some matrix multiplication and addition involving the results of the previous training and the new bias $\tilde{\boldsymbol{\theta}}^0$.

4.4. General convex regularization functions. So far, we have only considered quadratic regularizations. In this section, we will consider the linear regression problem with an arbitrary convex regularization term. Specifically, consider the general regularization term $R(\boldsymbol{\theta}) - \langle \mathbf{x}, \boldsymbol{\theta} \rangle$, where $R : \mathbb{R}^n \rightarrow \mathbb{R}$ is a convex function. Then, the loss function of the learning problem is given by

$$(4.6) \quad \mathcal{L}(\boldsymbol{\theta}) = \frac{1}{2} \sum_{i=1}^N \lambda_i \|\Phi_i \boldsymbol{\theta} - \mathbf{y}_i\|_2^2 + R(\boldsymbol{\theta}) - \langle \mathbf{x}, \boldsymbol{\theta} \rangle.$$

This learning problem corresponds to a multi-time HJ PDE (2.4), where the i -th Hamiltonian is $H_i(\mathbf{p}) = \frac{1}{2} \lambda_i \|\Phi_i \mathbf{p} - \mathbf{y}_i\|_2^2$ and the initial condition is $J = R^*$, which is the Fenchel-Legendre transform of R . The corresponding optimal control problem is given by (2.3), with terminal time $\sum_{i=1}^N \lambda_i$, piecewise running costs $L_i(\mathbf{u}) = \frac{1}{2} \|\mathbf{u}\|^2 - \langle \mathbf{y}_i, \mathbf{u} \rangle$ and piecewise dynamics $f_i(\mathbf{u}) = \Phi_i^T \mathbf{u}$ on $(\sum_{j=1}^{i-1} \lambda_j, \sum_{j=1}^i \lambda_j]$, and terminal cost R^* . Then, the solution $\boldsymbol{\theta}^*$ to the learning problem (4.6) is equivalent to the spatial gradient $\nabla_{\mathbf{x}} S(\mathbf{x}, \lambda_1, \dots, \lambda_N)$ of the solution to the multi-time HJ PDE, and the minimal value of the loss function (4.6) is equivalent to $-S(\mathbf{x}, \lambda_1, \dots, \lambda_N)$.

Since the loss function (4.6) is convex, it can be minimized using any appropriate convex optimization algorithm. In this paper, we demonstrate how our Riccati-based approach can be combined with PDHG [4] to solve this learning problem. Note that PDHG can be applied to this learning problem (4.6) as long as the proximal point of R or R^* is numerically computable. For instance, R could be a quadratic function $\langle \cdot, M \cdot \rangle$, a quadratic norm $\sqrt{\langle \cdot, M \cdot \rangle}$, $\|\cdot\|_1$, $\|\cdot\|_1^2$, $\|\cdot\|_\infty^2$, a polynomial function, or the Fenchel-Legendre transformation of any of these functions [10]. To compute the

solution $\boldsymbol{\theta}^*$ of this learning problem, PDHG iterates the following:

$$(4.7) \quad \begin{cases} \boldsymbol{\theta}^{\ell+1} = \arg \min_{\boldsymbol{\theta} \in \mathbb{R}^n} \frac{1}{2} \sum_{i=1}^N \lambda_i \|\Phi_i \boldsymbol{\theta} - \mathbf{y}_i\|_2^2 + \frac{1}{2\sigma_{\boldsymbol{\theta}}} \left\| \boldsymbol{\theta} - (\boldsymbol{\theta}^{\ell} - \sigma_{\boldsymbol{\theta}}(\mathbf{w}^{\ell} - \mathbf{x})) \right\|_2^2, \\ \bar{\boldsymbol{\theta}}^{\ell+1} = 2\boldsymbol{\theta}^{\ell+1} - \boldsymbol{\theta}^{\ell}, \\ \mathbf{w}^{\ell+1} = \arg \min_{\mathbf{w} \in \mathbb{R}^n} R^*(\mathbf{w}) + \frac{1}{2\sigma_{\mathbf{w}}} \left\| \mathbf{w} - (\mathbf{w}^{\ell} + \sigma_{\mathbf{w}} \bar{\boldsymbol{\theta}}^{\ell+1}) \right\|_2^2, \end{cases}$$

where $\sigma_{\boldsymbol{\theta}}, \sigma_{\mathbf{w}}$ are positive step-size parameters satisfying $\sigma_{\boldsymbol{\theta}}\sigma_{\mathbf{w}} < 1$. In each iteration, we need to solve two minimization problems. Updating $\boldsymbol{\theta}^{\ell}$ is equivalent to solving the learning problem with quadratic regularization. Specifically, updating $\boldsymbol{\theta}^{\ell}$ is the same as changing the bias θ^0 in the loss function (4.1). Therefore, we only need to solve the Riccati ODEs (4.2) once (to compute $\boldsymbol{\theta}^1$) and every other iterate can be computed using (4.5). Updating \mathbf{w}^{ℓ} is equivalent to computing the proximal point of R^* . Depending on R^* , there may already exist efficient solvers or explicit formulas for computing its proximal point.

Note that with non-quadratic regularization, if we change the weights λ_k of the data fitting losses, change \mathbf{x} (which is related to the bias on $\boldsymbol{\theta}$), or add or remove data points, then we will need to restart PDHG to solve the resulting learning problem with these new hyper-parameter values or updated datasets. However, we can reuse some of the computations between runs. Namely, we only need to solve the full sequence of Riccati ODEs (4.2) once (to compute $\boldsymbol{\theta}^1$ in the first run of PDHG). Then, the solution to those Riccati ODEs can be reused in combination with the methods described in Sections 4.2 and 4.3 (according to how the learning problem is modified) in subsequent iterations and runs of PDHG.

5. Numerical examples. In this section, we apply the Riccati-based methodology presented in Section 4 to four test problems from machine learning to demonstrate the versatility and potential computational advantages of our new approach. In each example, we use RK4 with double precision to solve the Riccati ODEs when applying our Riccati-based methodology. The connections between the examples presented in this section, the Hopf formula, and the corresponding optimal control problems can be found in Table 1.

5.1. Function approximation in continual learning. In this section, we test our Riccati-based approach (as described in Section 5.1) on a pedagogical function approximation example in continual learning [26, 19, 33] to demonstrate its computational and memory advantages. Under the continual learning framework, data is accessed in a stream and the trainable model parameters are updated incrementally as new data becomes available. In some cases, the historical data may also become inaccessible after new data is received, which can often lead to catastrophic forgetting [19, 26], which refers to the abrupt degradation in performance of learned models on previous tasks upon training on new tasks. In this example, we show how our Riccati-based approach naturally coincides with the continual learning framework, while also inherently avoiding catastrophic forgetting even if the historical data is inaccessible.

Our example set-up is as follows. Our goal is to regress the function $y(\tau) = 0.1\tau + 0.05 \sin(10\tau)$ given noisy data $\{(\tau_i, y_i \approx y(\tau_i))\}_{i=1}^N \subset \mathbb{R} \times \mathbb{R}$. Following the continual learning framework, we assume that a new noisy data point is available every $\Delta\tau = 0.01$ (i.e., $\tau_i = (i-1)\Delta\tau \in [0, 10]$, $i = 1, \dots, N$). We regress $y(\tau)$ using the linear model $y(\tau) = \sum_{k=1}^n \theta_k \phi_k(\tau)$, where $n = 10$ and the basis functions are

given by

$$(5.1) \quad \{\phi_k(\tau)\}_{k=1}^n = \{1, \tau, \tau^2, \tau^3, \sin(\tau), \sin(5\tau), \sin(8\tau), \sin(9\tau), \sin(10\tau), \sin(12\tau)\}.$$

The coefficients $\boldsymbol{\theta} = [\theta_1, \dots, \theta_n]^T$ of our linear model are learned by minimizing the following loss function:

$$(5.2) \quad \mathcal{L}(\boldsymbol{\theta}) = \frac{1}{2} \sum_{i=1}^N \lambda_i \left| \sum_{k=1}^n \theta_k \phi_k(\tau_i) - y_i \right|^2 + \frac{1}{2} \sum_{k=1}^n \gamma_k |\theta_k|^2,$$

where $\lambda_i, i = 1, \dots, N$ and $\gamma_k, k = 1, \dots, n$ are weights for the data loss and ℓ_2 regularization terms, respectively, and we update our learned coefficients every time a new data point is available. In our numerical experiments, we use additive Gaussian noise with zero mean and standard deviation 0.01, and we set $\lambda_i = 1, \forall i$ and $\gamma_k = 0.1, \forall k$.

Although this loss function (5.2) could be minimized using conventional machine learning techniques (e.g., the method of least squares), these methods typically require access to and training on the entire dataset $\{(\tau_i, y_i)\}_{i=1}^N$, which conflicts with the assumptions in continual learning. However, note that this loss function (5.2) is of the form (4.1). Thus, we can instead apply our Riccati-based approach (as described in Sections 4.1 and 4.2) to solve this learning problem. In particular, the methodology described in Section 4.2 matches the data streaming paradigm of continual learning; we incrementally update our learned coefficients by considering each new data point as the time evolution of a corresponding multi-time HJ PDE. As a result, in contrast to conventional machine learning methods, our Riccati-based approach does not require storage of previous data points and its memory and computational complexity is constant for each added data point. As such, our Riccati-based methodology may be well-suited to online learning applications. Additionally, since this time evolution of the HJ PDE (i.e., the addition of a new data point) requires knowledge about the solution to the HJ PDE at the previous time (i.e., the results of the previous training), our Riccati-based approach also inherently avoids catastrophic forgetting.

The results of applying our Riccati-based method to solve this learning problem (5.4) are shown in Figure 6 and Table 2. Figure 6(a) depicts the evolution of the coefficients $\{\theta_k\}_{k=1}^n$ as more data points become available. We observe that the learned coefficients $\theta_k, k = 1, \dots, n$ converge to their true values as more data points are incorporated into the model. Figure 6(b) displays three inferences at different times $\tau = 2, 4, 8$, which demonstrate that our Riccati-based approach is capable of real-time inferences without catastrophic forgetting, even though each inference is made using only one data point. Note that due to an appropriate choice of basis functions, our learned model is able to provide accurate extrapolations as well.

Table 2 displays the numerical errors of the minimizer $\boldsymbol{\theta}^*$ of the loss function (5.2) obtained using the Riccati-based methodology from Section 4 after the last data point becomes available at $\tau = 10$. We observe that the accuracy of our approach increases as we decrease the step size h of RK4, which indicates that the errors of $\boldsymbol{\theta}^*$ stem from the accuracy of RK4 in solving the corresponding Riccati ODEs. The reference solution is obtained by minimizing (5.2) directly using the method of least squares and assuming that all $N = 1000$ data points are accessible.

5.2. 1D steady-state reaction-diffusion equation and post-training calibration. In this example, we use our Riccati-based approach to apply post-training calibrations when solving a PDE. Specifically, we leverage the methodology in Section 4.2 to add or remove data and the methodology in Sections 4.3 to enforce the

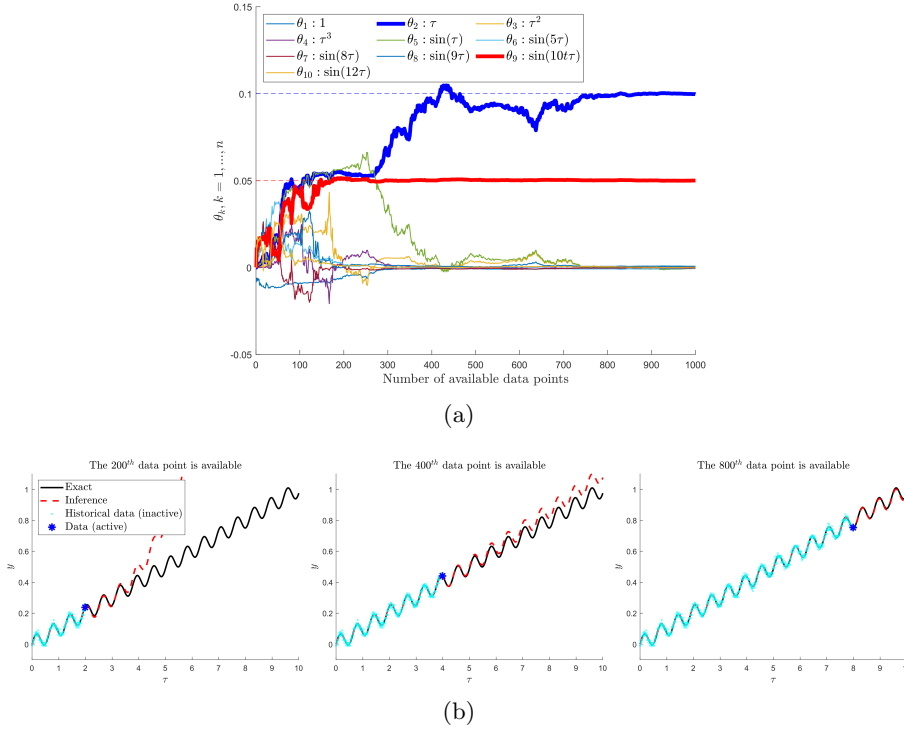


Fig. 6: Evolution and continual learning of the function approximation learned using our Riccati-based approach as more data becomes available. (a) shows the evolution of the learned coefficients $\theta_k, k = 1, \dots, n$ as more data is incorporated into the model; the horizontal dotted lines denote the exact reference values. (b) shows the inferences of y after the 200th, 400th, and 800th noisy data point becomes available. Our Riccati-based approach allows us to incrementally update the learned coefficients as more data becomes available without requiring access to the previous data or re-training on the entire dataset, which provides advantages in both memory and computations over conventional learning methods.

boundary conditions of the PDE without retraining the entire learned model. Consider the following 1D steady-state reaction-diffusion equation:

$$(5.3) \quad \begin{cases} D \frac{\partial^2 u}{\partial x^2}(x) + \kappa u(x) = f(x), x \in [0, 1], \\ u(0) = u(1) = 0, \end{cases}$$

where $D = 0.01$ is the diffusion coefficient, $\kappa = -1$, and $f(x)$ is the source term of which noisy measurements $\{(x_i, f_i \approx f(x_i))\}_{i=1}^N \subset \mathbb{R} \times \mathbb{R}$ are available. We consider the scenario where regular training has been employed but with either insufficient data or sufficient data with outliers, both of which yield inaccurate inferences of the solution. We further assume that extra information is provided after the regular training and seek to perform post-training calibrations to incorporate this extra information into the already-trained models without losing the information from the

	$h = 0.2$	$h = 0.1$	$h = 0.01$
ℓ_1 error of θ^*	1.1210×10^{-6}	6.0924×10^{-9}	4.2222×10^{-12}
ℓ_1 relative error of θ^*	7.3622×10^{-6}	4.0012×10^{-8}	2.7729×10^{-11}

Table 2: Errors in computing the minimizer θ^* of the function approximation loss (5.2) using our Riccati-based approach. We use RK4 to solve the Riccati ODEs (4.2) and (4.3) with double precision and various step sizes h . The reference is obtained by using the method of least squares to minimize the loss function (5.2) directly.

original training. In the literature, it is well-established that post-training calibration can significantly increase the performance of deployed machine learning methods [27, 37]. However, designing computationally efficient methods for performing these post-calibrations is still of great interest.

In this example, we solve this PDE (5.3) by reformulating the PDE as an optimization problem [28, 31, 15]. We use a linear model to approximate the solution, i.e. $u(x) = \sum_{k=1}^n \theta_k \phi_k(x)$, where $n = 21$ and $\{\phi_k(x)\}_{k=1}^n$ are the truncated Fourier basis functions on $[0, 1]$, $\{1\} \cup \{\sin(2l\pi x), \cos(2l\pi x)\}_{l=1}^{(n-1)/2}$. We learn the coefficients $\theta = [\theta_1, \dots, \theta_n]^T$ of the linear model by minimizing the following loss:

$$(5.4) \quad \mathcal{L}(\theta) = \frac{1}{2} \sum_{i=1}^N \lambda_i \left| D \sum_{k=1}^n \theta_k \frac{\partial^2 \phi}{\partial x^2}(x_i) + \kappa \sum_{k=1}^n \theta_k \phi_k(x_i) - f_i \right|^2 + \frac{1}{2} \lambda_b \left| \sum_{k=1}^n \theta_k \phi_k(0) - 0 \right|^2 + \frac{1}{2} \lambda_b \left| \sum_{k=1}^n \theta_k \phi_k(1) - 0 \right|^2 + \frac{1}{2} \sum_{k=1}^n \gamma_k |\theta_k|^2,$$

where $\lambda_i, i = 1, \dots, N$, λ_b , and $\gamma_k, k = 1, \dots, n$ are balancing weights for the PDE residual, the boundary conditions, and the regularization term, respectively. In our numerical experiments, we assume the exact solution to be $u(x) = \sin^3(2\pi x)$ (and f to be defined by (5.3), accordingly) and the noise to be additive Gaussian with zero mean and standard deviation 0.1. For the regular training, we set $\lambda_i = 1$, $\lambda_b = 1$, and $\gamma_k = 1$ and apply our Riccati-based method (see Section 4.1) to get our original estimate of the minimizer θ^* of the loss function (5.4). Using our Riccati-based method yields an ℓ_1 error of 8.9154×10^{-10} and relative ℓ_1 error of 1.4162×10^{-9} in θ^* , where the reference is obtained by minimizing (5.4) directly using the method of least squares.

In the leftmost column of Figure 7, we see that the accuracy of both u and f as inferred by the regular training is impaired by a lack of data around the highest peak and lowest valley of the exact functions. To compensate, we first calibrate our model by adding some new noisy measurements of f in these regions where the data points are sparse. This calibration uses the methodology described in Section 4.2, and the results are shown in the middle column of Figure 7. Next, we note that the inferred u still disagrees with the exact solution at the boundary points. Hence, we further calibrate our model by increasing the value of the boundary weight λ_b from 1 to 10 to enforce the boundary conditions of the PDE. This calibration is done using the methodology described in Section 4.3 and the results of this second calibration are presented in the rightmost column of Figure 7. In both cases, we observe that the calibrations successfully improve the accuracy of the learned model.

Note that our Riccati-based approach allows us to perform each of these calibration steps using only the new or changed values in that step and the results of the previous training step. In other words, each step of this training process (including the

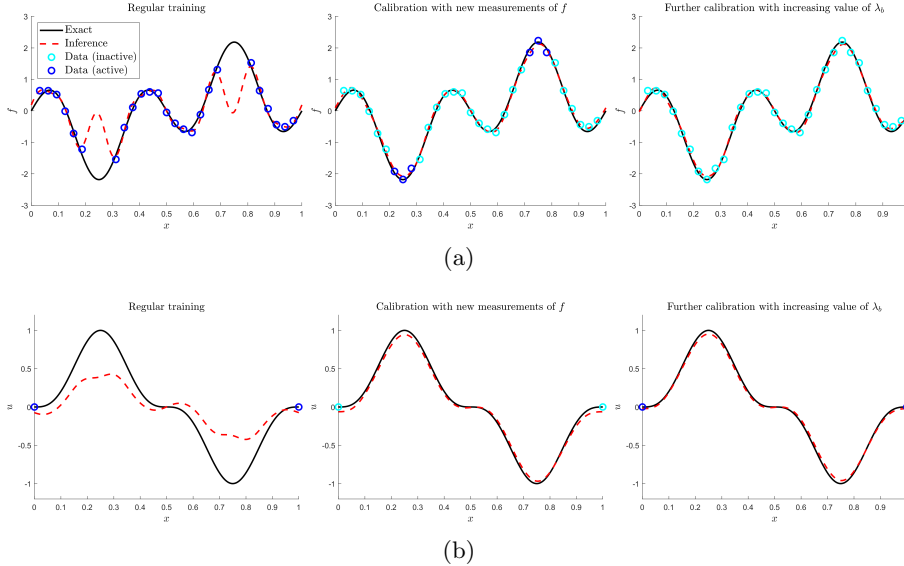


Fig. 7: Results of solving the 1D steady-state reaction-diffusion equation (5.3) with noisy measurements of the source term f in the domain and noiseless measurements of the solution u on the boundary. (a) results for f ; (b) results for u . **Left**: results of regular training; **middle**: calibrating the results of regular training with some additional noisy measurements of f ; **right**: calibrating the results further by enforcing the boundary conditions by increasing the value of λ_b in the loss function (5.4). The regular training uses our Riccati-based method in Section 4.1 to minimize (5.4), while the calibrations use the adaptations of our method in Section 4.2. Calibrations are employed without re-training or access to the data from the previous training, which demonstrates the advantages in both memory storage and computational complexity of our Riccati-based approach over conventional machine learning methods.

original training and each subsequent calibration step) is done without sharing data between training steps, which exactly matches the framework of federated learning [21]. Thus, our methodology may be relevant to distributed training or collaborative learning applications, where data privacy is of concern.

Next, we discuss another post-training calibration technique. In this case, we assume the data for the regular training is sufficient but contains outliers due to large noise. We again assume the regular training is performed using the Riccati-based approach from Section 4.1. Then, we eliminate these outliers using the methodology described in Section 4.2, which only requires knowledge about the outliers to be removed and the results of the regular training. The results of this post-training outlier removal show that eliminating these points successfully improves the accuracy of the learned models (see Appendix B).

5.3. Poisson equation using PINNs and transfer learning. In this example, we demonstrate the versatility of our Riccati-based method by combining it with existing machine learning techniques to fit the last layer of a PINN. We also show that when we perform hyper-parameter tuning by solving the associated Riccati

ODEs (Section 4.3), we not only provide the solution to the updated problem, but also a continuum of solutions along a 1D curve on the Pareto front of the data fitting losses and regularization. Consider the 2D Poisson equation with Dirichlet boundary conditions is given by

$$(5.5) \quad \begin{cases} \frac{\partial^2 u}{\partial x^2}(x, y) + \frac{\partial^2 u}{\partial y^2}(x, y) = f(x, y) & (x, y) \in \Omega, \\ u(x, y) = 0 & (x, y) \in \partial\Omega, \end{cases}$$

where $\Omega := [-1, 1]^2$ and f is a source term. In this example, we solve this equation using transfer learning and PINNs. Consider the scenario where we only have access to measurements $\{(x_i, y_i, f_i = f(x_i, y_i))\}_{i=1}^N$ of f at limited sampling points. Transfer learning compensates for this lack of knowledge, by transferring the knowledge from models pre-trained on similar problems to solve this new problem of interest. In this case, we learn the linear model $u(x, y) = \sum_{k=1}^n \theta_k \phi_k(x, y)$, where each basis function $\phi_k(x, y), k = 1, \dots, n$ is the PINN solution of a neural network pre-trained to solve the 2D Poisson equation (5.5) with similar source terms. Transfer learning using pre-trained neural networks as basis functions, as we do here, has recently grown in popularity in the scientific machine learning community [11, 36, 14] and has been shown to provide efficient yet accurate inferences even given very limited data [36]. We then learn the coefficients $\boldsymbol{\theta}$ of our linear model by minimizing the following PINN-type loss:

$$(5.6) \quad \mathcal{L}(\boldsymbol{\theta}) = \frac{1}{2} \sum_{i=1}^N \lambda_i \left| \sum_{k=1}^n \theta_k \left(\frac{\partial^2 \phi_k}{\partial x^2} + \frac{\partial^2 \phi_k}{\partial y^2} \right) (x_i, y_i) - f_i \right|^2 + \frac{1}{2} \sum_{k=1}^n \gamma_k |\theta_k|^2,$$

where $\lambda_i = 1, i = 1, \dots, N$ and $\gamma_k = \gamma, k = 1, \dots, n$ are weights for the data fitting and ℓ_2 -regularization terms, respectively. Note that minimizing (5.6) with respect to $\boldsymbol{\theta}$ is equivalent to fitting the last layer of a neural network given pre-trained previous nonlinear layers as the basis functions.

In our numerical experiments, we use transfer learning to solve the 2D Poisson equation (5.5) with source term $f(x, y) = \sin(2.5\pi x) \sin(2.5\pi y)$ using $n = 100$ basis functions and $N = 100$ random measurements of f . We use the multi-head PINN method [36] to obtain the basis functions, which correspond to the shared nonlinear hidden layers of the pre-trained PINN solutions to (5.5) with source terms $f(x, y) = \sin(k\pi x) \sin(k\pi y), k = 1, 2, 3, 4$. We solve the learning problem (5.6) using our Riccati-based method from Section 4.1.

In Table 3, we compare the errors of the minimizer $\boldsymbol{\theta}^*$ of (5.6) and the solution u of the PDE (5.5) as we decrease the weight $\gamma (= \gamma_k, \forall k)$ of the regularization term from 1 to 1e-5. The reference for $\boldsymbol{\theta}^*$ is obtained from minimizing (5.6) directly for each value of γ using the method of least squares. The reference for u is computed using a finite difference method with a five-point stencil to solve (5.5). Note that we originally minimize (5.6) using $\gamma = 1$ and the Riccati-based method in Section 4.1. We then compute the solutions for the other values of γ by incrementally decreasing γ by a factor of 10 and using the methodology for hyper-parameter tuning described in Section 4.3 to reuse the results of training with the previous value γ to compute the solution for the new value of γ . Consequently, we see that the error in $\boldsymbol{\theta}^*$ increases as we decrease γ due to error accumulation from repeated applications of RK4. However, we also see that the error of u generally decreases as we decrease γ with the lowest error being achieved when $\gamma = 1e-4$.

	$\gamma = 1$	$\gamma = 0.1$	$\gamma = 0.01$	$\gamma = 0.001$	$\gamma = 0.0001$	$\gamma = 0.00001$
ℓ_1 error of θ^*	5.9707×10^{-10}	4.2905×10^{-8}	1.0725×10^{-6}	1.7235×10^{-5}	2.0490×10^{-4}	5.8749×10^{-3}
L^2 relative error of u	6.5247%	5.6793%	3.0390%	1.7280%	1.1662%	1.4736%

Table 3: Errors of the minimizer θ^* of (5.6) and the solution u to the 2D Poisson equation (5.5) using transfer learning and our Riccati-based approach. The reference for θ^* is given by minimizing (5.6) with the corresponding value of γ directly using the method of least squares, and the reference for u is given by solving (5.5) using a finite difference method. Since we decrease γ incrementally from 1 to 1e-5, the error of θ^* accumulates due to successive applications of RK4.

From the results in Table 3, we see that our choice of the hyper-parameter γ can greatly influence the accuracy of our learned model. Note that since we fix $\lambda_i = 1, \forall i$ and $\gamma_k = \gamma, \forall k$, we can view (5.6) as a bi-objective loss, where the two objectives are the weighted data fitting term $\frac{1}{2} \sum_{i=1}^N \left| \sum_{k=1}^n \theta_k \left(\frac{\partial^2 \phi_k}{\partial x^2} + \frac{\partial^2 \phi_k}{\partial y^2} \right) (x_i, y_i) - f_i \right|^2$ and the regularization term $\frac{1}{2} \sum_{k=1}^n |\theta_k|^2$. To better understand the effects of tuning γ , in Figure 8, we explore the Pareto front of these two objectives. Traditional scalarization-based approaches for computing the Pareto front typically rely on discrete samplings of the Pareto front corresponding to discrete choices of γ [17]. While our Riccati-based methodology from Section 4.3 also recovers discrete points on the Pareto front corresponding to particular choices of γ , note that when we change γ , e.g., from $\gamma = 1$ to $\gamma = 0.1$, we also recover a one-dimensional curve along the Pareto front corresponding to every $\gamma \in [0.1, 1]$. We obtain this 1D curve theoretically via the flow of solutions obtained from the corresponding Riccati ODEs and numerically via the intermediate steps of RK4. The left plot of Figure 8 shows the 1D curve along the Pareto front recovered by our Riccati-based approach (although note that in this example, the Pareto front is also one-dimensional and hence is equivalent to the exposed 1D curve), where the flow of solutions corresponding to decreasing γ is represented by the arrows. Thus, although in general our methodology cannot compute the entire Pareto front, every time we change the value of the hyper-parameters, our approach recovers a continuous 1D curve along the Pareto front. In the right plot of Figure 8, we also visualize how the L^2 error of our learned solution u changes as we decrease γ .

5.4. Identifying the dynamics of the Kraichnan-Orszag system from data. In this example, we demonstrate the versatility of our Riccati-based approach by showing how it can be combined with existing methods to solve more general problems (see Section 4.4). Consider the Kraichnan-Orszag (K-O) system [34, 37]:

$$(5.7) \quad \begin{cases} \frac{dx_1}{d\tau} = x_2 x_3, \\ \frac{dx_2}{d\tau} = x_1 x_3, \\ \frac{dx_3}{d\tau} = -2x_1 x_2, \end{cases}$$

with initial conditions $x_1(0) = 1, x_2(0) = 0.8, x_3(0) = 0.5$. Our goal is to identify the dynamics of the K-O system (i.e. the right-hand side of (5.7)) using measurements of x_i and $\frac{dx_i}{d\tau}, i = 1, 2, 3$ at different times. We identify the dynamics by learning the linear models $\frac{dx_i}{d\tau} = \sum_{k=1}^n \theta_k^i \phi_k, i = 1, 2, 3$. Following the general framework of the SINDy method [2], we use the following quadratic basis functions ($n = 10$) for the

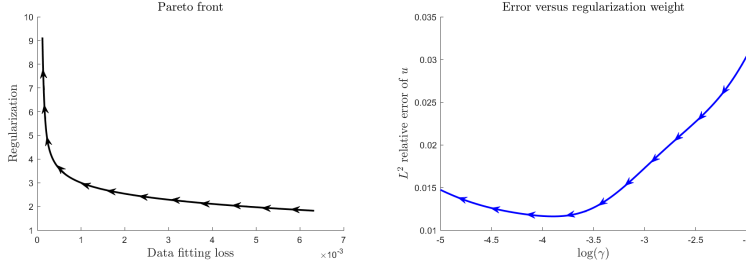


Fig. 8: Results of changing the regularization weight γ when solving the 2D Poisson equation using PINNs and transfer learning. We incrementally decrease the value of γ by evolving the corresponding Riccati ODEs backwards in time. As a result, we obtain a flow of solutions, the direction of which is represented by the arrows in each figure. In the left figure, this flow of solutions gives us that every change in the value of γ from $\hat{\gamma}$ to $\tilde{\gamma}$ results in the recovery of every point of the Pareto front along the one-dimensional curve parameterized by $\gamma \in [\hat{\gamma}, \tilde{\gamma}]$.

dynamics:

$$(5.8) \quad \{\phi_k(x_1, x_2, x_3)\}_{k=1}^n = \{1, x_1, x_2, x_3, x_1^2, x_2^2, x_3^2, x_1x_2, x_2x_3, x_1x_3\},$$

and impose ℓ_1 -regularization on θ to promote sparse identification of the dynamics. Then, we learn each θ^i independently and in parallel by minimizing the loss functions

$$(5.9) \quad \mathcal{L}_i(\theta^i) = \frac{1}{2} \sum_{j=1}^N \lambda_j \left[\left(\frac{dx_i}{d\tau} \right)_j - \sum_{k=1}^n \theta_k^i \phi_k((x_1)_j, (x_2)_j, (x_3)_j) \right]^2 + \sum_{k=1}^n \gamma_k |\theta_k^i|,$$

where \mathcal{L}_i denotes the loss function for equation i , $(x_i)_j$ and $(\frac{dx_i}{d\tau})_j$ denote the measurements of x_i and $\frac{dx_i}{d\tau}$, respectively, at time τ_j , $i = 1, 2, 3, j = 1, \dots, N$. Note that this loss function (5.9) corresponds to setting $R = \|\cdot\|_1$ and $\mathbf{x} = 0$ in the linear regression problem (4.6). Thus, solving this learning problem is equivalent to evaluating the solution to the corresponding multi-time HJ PDE at $(0, \lambda_1, \dots, \lambda_n)$. In our numerical experiments, we generate data points for training and testing by solving (5.7) numerically for $x_1, x_2, x_3 \in [0, 10]$ using a central finite difference scheme to approximate the time derivatives, and set $\lambda_j = 1, \forall j$ and $\gamma_k = 0.1, \forall k$.

Instead of the sparse regression techniques employed by SINDy, we use PDHG to minimize (5.9) (see Section 4.4). Each iteration of PDHG involves minimizing a loss function of the form (5.9), but with ℓ_2 -regularization instead of ℓ_1 . Hence, this subproblem can be solved using our Riccati-based methods. As discussed in Section 4.4, note that we only need to apply RK4 for the first iteration of PDHG, and every subsequent iteration can be solved using a change of bias. As such, we do not suffer from any error accumulation related to repeated applications of RK4. In Table 4, we see that we do indeed recover a sparse identification of the dynamics. However, we also incorrectly identify non-zero coefficients for the basis functions x_2 and x_3 . We note that this misidentification may be the result of a lack of unique identifiability of the system from the data points sampled. In fact, Table 5 shows that the errors in the solution x_1, x_2, x_3 of the identified system versus the solution of the true system (5.7) are relatively small, which corroborates that identifiability may have been an issue.

	1	x_1	x_2	x_3	x_1^2	x_2^2	x_3^2	x_1x_2	x_2x_3	x_1x_3
$\theta^{1,*}$	0	0	0	0	0	0	0	0	0.9931	0
$\theta^{2,*}$	0	0	0	0.0160	0	0	0	0	0	0.9761
$\theta^{3,*}$	0	0	-0.0165	0	0	0	0	-1.9777	0	0

Table 4: Results of sparse identification of the K-O system (5.7) using PDHG to minimize the ℓ_1 -regularized losses (5.9). The true solution is 0 for all entries, except $\theta^{1,*} = 1$ for x_2x_3 , $\theta^{2,*} = 1$ for x_1x_3 , and $\theta^{3,*} = -2$ for x_1x_2 . We recover the dynamics reasonably well, albeit with some slight misidentification of $\theta^{2,*}$, $\theta^{3,*}$.

	x_1	x_2	x_3
relative L^2 error (%)	0.2144	0.3718	0.3152

Table 5: Errors of the solution x_1, x_2, x_3 of the system identified using PDHG compared to the true solution of the K-O system. The reference is obtained by numerically solving the true system (5.7) using a central finite difference scheme. These errors indicate that the errors in the system identification in Table 4 may be due to a lack of unique identifiability of the system using the given data points.

6. Summary. In this paper, we established a novel theoretical connection between certain learning problems and the multi-time Hopf formula. In doing so, we showed that when we solve certain learning problems, we actually solve certain multi-time HJ PDEs and their corresponding optimal control problems. In this work, we focused on the development of the connection between regularized linear regression and the LQR problem. By leveraging this novel connection, we developed new methodology based on solving Riccati ODEs that allows us to design novel training approaches for certain machine learning applications, including continual learning, post-training calibration, hyper-parameter tuning and exploration of the associated Pareto front, and sparse dynamics identification. We also showed that our Riccati-based approach yields some promising computational advantages over conventional learning methods; after the original training, the models learned using our approach can be continually updated without having to retrain the entire model or having access to all of the previous data, which could be particularly useful in continual learning [26, 19, 33] and federated learning [21, 18].

Thus, our novel theoretical connection and our Riccati-based methodology present many exciting opportunities. Some possible future directions are as follows. While our Riccati-based methodology allows us to alter the hyper-parameters and data points used in the learning problem without having to retrain on all previous data, it also requires that the original training be done using our Riccati-based methodology. It would allow for increased versatility if we could more easily combine our Riccati-based approach with other training methods. Additionally, in Sections 4.4 and 5.4, we showed that our Riccati-based approach allows computations to be reused when using non-quadratic regularizations. However, in this case, the training process still had to be restarted if the hyper-parameters, dataset, or regularization type is changed. It would allow for more flexibility if we could develop more adaptive processes for changing these aspects of the learning problem when the regularization is not quadratic.

In Section 3, we focused on LQR problems, where the dynamics are independent of the trajectory, but it would be worthwhile to investigate what connections

LQR problems with general linear dynamics may yield (e.g., LQR problems with general linear dynamics may be reformulated as LQR problems with state-independent dynamics using a change of variable [10]). Another natural extension would be to consider nonlinear models, which currently pose challenges in both scientific machine learning and optimal control and hence, connections drawn in this case would benefit both fields. Alternatively, if we relax our assumption on convexity by allowing for nonconvex loss functions (or equivalently, nonconvex Hamiltonians), we could also extend our connection to be between learning problems and differential games [12] instead of optimal control. However, even with convex losses, there are already many interesting potential applications in machine learning to pursue. For example, the theoretical connection presented in Section 2.2 provides a formula for the optimal learning parameters θ^* in terms of the hyper-parameters. This connection could be leveraged to simplify the bi-level optimization in meta-learning applications to a single-level, constrained optimization problem. As another example, we could generalize our theory to instead consider the viscous HJ PDE, which adds a Laplacian term to the right-hand side of the HJ PDEs (2.1) and (2.4). Then, by leveraging the recently established connection between viscous HJ PDEs and Bayesian modeling [7], we could extend our work to applications in Bayesian inference.

Acknowledgments. P.C. is supported by the SMART Scholarship, which is funded by the Under Secretary of Defense/Research and Engineering (USD/R&E), National Defense Education Program (NDEP) / BA-1, Basic Research. J.D., G.E.K., and Z.Z. are supported by the MURI/AFOSR FA9550-20-1-0358 project.

REFERENCES

- [1] M. BARDI AND I. CAPUZZO-DOLCETTA, *Optimal control and viscosity solutions of Hamilton-Jacobi-Bellman equations*, Systems & Control: Foundations & Applications, Birkhäuser Boston, Inc., Boston, MA, 1997, <https://doi.org/10.1007/978-0-8176-4755-1>, <https://doi.org/10.1007/978-0-8176-4755-1>. With appendices by Maurizio Falcone and Pierpaolo Soravia.
- [2] S. L. BRUNTON, J. L. PROCTOR, AND J. N. KUTZ, *Discovering governing equations from data by sparse identification of nonlinear dynamical systems*, Proceedings of the National Academy of Sciences, 113 (2016), pp. 3932–3937.
- [3] J. C. BUTCHER, *Numerical methods for ordinary differential equations*, John Wiley & Sons, 2016.
- [4] A. CHAMBOLLE AND T. POCK, *A first-order primal-dual algorithm for convex problems with applications to imaging*, Journal of Mathematical Imaging and Vision, 40 (2011), pp. 120–145.
- [5] J. DARBON, *On convex finite-dimensional variational methods in imaging sciences and Hamilton–Jacobi equations*, SIAM Journal on Imaging Sciences, 8 (2015), pp. 2268–2293, <https://doi.org/10.1137/130944163>, <https://arxiv.org/abs/https://doi.org/10.1137/130944163>.
- [6] J. DARBON, P. M. DOWER, AND T. MENG, *Neural network architectures using min-plus algebra for solving certain high-dimensional optimal control problems and Hamilton–Jacobi PDEs*, Math. Control Signals Systems, 35 (2023), pp. 1–44, <https://doi.org/10.1007/s00498-022-00333-2>, <https://doi.org/10.1007/s00498-022-00333-2>.
- [7] J. DARBON AND G. LANGLOIS, *On Bayesian Posterior Mean Estimators in Imaging Sciences and Hamilton–Jacobi Partial Differential Equations*, J. Math Imaging Vis., 63 (2021), p. 821–854.
- [8] J. DARBON AND T. MENG, *On decomposition models in imaging sciences and multi-time Hamilton–Jacobi partial differential equations*, SIAM Journal on Imaging Sciences, 13 (2020), pp. 971–1014, <https://doi.org/10.1137/19M1266332>, <https://doi.org/10.1137/19M1266332>, <https://arxiv.org/abs/https://doi.org/10.1137/19M1266332>.
- [9] J. DARBON, T. MENG, AND E. RESMERITA, *On Hamilton–Jacobi PDEs and Image Denoising Models with Certain Nonadditive Noise*, Journal of Mathematical Imaging and Vision, 64

- (2022), p. 408–441.
- [10] J. DARBON AND S. OSHER, *Algorithms for overcoming the curse of dimensionality for certain Hamilton-Jacobi equations arising in control theory and elsewhere*, Res Math Sci Research in the Mathematical Sciences, 3 (2016), pp. 1–26, <https://doi.org/10.1186/s40687-016-0068-7>, <https://doi.org/10.1186/s40687-016-0068-7>.
- [11] S. DESAI, M. MATTHEAKIS, H. JOY, P. PROTOPAPAS, AND S. ROBERTS, *One-shot transfer learning of physics-informed neural networks*, arXiv preprint arXiv:2110.11286, (2021).
- [12] L. C. EVANS AND P. E. SOUGANIDIS, *Differential games and representation formulas for solutions of Hamilton-Jacobi-Isaacs equations*, Indiana University mathematics journal, 33 (1984), pp. 773–797.
- [13] I. GOODFELLOW, Y. BENGIO, AND A. COURVILLE, *Deep learning*, MIT press, 2016.
- [14] S. GOSWAMI, K. KONTOLATI, M. D. SHIELDS, AND G. E. KARNIADAKIS, *Deep transfer operator learning for partial differential equations under conditional shift*, Nature Machine Intelligence, (2022), pp. 1–10.
- [15] J. HAN, A. JENTZEN, AND W. E, *Solving high-dimensional partial differential equations using deep learning*, Proceedings of the National Academy of Sciences, 115 (2018), pp. 8505–8510.
- [16] E. HOPF, *Generalized Solutions of non-linear Equations of First Order*, Journal of Mathematics and Mechanics, 14 (1965), pp. 951–973.
- [17] Y. JIN AND B. SENDHOFF, *Pareto-based multiobjective machine learning: An overview and case studies*, IEEE Transactions on Systems, Man, and Cybernetics, Part C (Applications and Reviews), 38 (2008), pp. 397–415, <https://doi.org/10.1109/TSMCC.2008.919172>.
- [18] P. KAIROUZ, H. B. MCMAHAN, B. AVENT, A. BELLET, M. BENNIS, A. N. BHAGOJI, K. BONAWITZ, Z. CHARLES, G. CORMODE, R. CUMMINGS, ET AL., *Advances and open problems in federated learning*, Foundations and Trends® in Machine Learning, 14 (2021), pp. 1–210.
- [19] J. KIRKPATRICK, R. PASCANU, N. RABINOWITZ, J. VENESS, G. DESJARDINS, A. A. RUSU, K. MILAN, J. QUAN, T. RAMALHO, A. GRABSKA-BARWINSKA, ET AL., *Overcoming catastrophic forgetting in neural networks*, Proceedings of the National Academy of Sciences, 114 (2017), pp. 3521–3526.
- [20] Y. LECUN, Y. BENGIO, AND G. HINTON, *Deep learning*, Nature, 521 (2015), pp. 436–444.
- [21] T. LI, A. K. SAHU, A. TALWALKAR, AND V. SMITH, *Federated learning: Challenges, methods, and future directions*, IEEE Signal Processing Magazine, 37 (2020), pp. 50–60.
- [22] P. L. LIONS AND J.-C. ROCHET, *Hopf Formula and Multitime Hamilton-Jacobi Equations*, Proceedings of the American Mathematical Society, 96 (1986), pp. 79–84, <http://www.jstor.org/stable/2045657>.
- [23] W. MCENEANEY, *Max-plus methods for nonlinear control and estimation*, Springer Science & Business Media, 2006.
- [24] M. MOHRI, A. ROSTAMIZADEH, AND A. TALWALKAR, *Foundations of machine learning*, MIT press, 2018.
- [25] T. NAKAMURA-ZIMMERER, Q. GONG, AND W. KANG, *QRnet: optimal regulator design with LQR-augmented neural networks*, IEEE Control Syst. Lett., 5 (2021), pp. 1303–1308.
- [26] G. I. PARISI, R. KEMKER, J. L. PART, C. KANAN, AND S. WERMTER, *Continual lifelong learning with neural networks: A review*, Neural networks, 113 (2019), pp. 54–71.
- [27] A. F. PSAROS, X. MENG, Z. ZOU, L. GUO, AND G. E. KARNIADAKIS, *Uncertainty quantification in scientific machine learning: Methods, metrics, and comparisons*, Journal of Computational Physics, (2023), p. 111902.
- [28] M. RAISSI, P. PERDIKARIS, AND G. KARNIADAKIS, *Physics-informed neural networks: A deep learning framework for solving forward and inverse problems involving nonlinear partial differential equations*, Journal of Computational Physics, 378 (2019), pp. 686–707.
- [29] J.-C. ROCHET, *The taxation principle and multi-time Hamilton-Jacobi equations*, Journal of Mathematical Economics, 14 (1985), pp. 113–128.
- [30] S. J. RUSSELL, *Artificial intelligence: A modern approach*, Pearson Education, Inc., 2010.
- [31] J. SIRIGNANO AND K. SPILIOPOULOS, *DGM: A deep learning algorithm for solving partial differential equations*, Journal of Computational Physics, 375 (2018), pp. 1339–1364.
- [32] H. L. TRENTELMAN, A. A. STOORVOGEL, AND M. HAUTUS, *Control Theory for Linear Systems*, Springer-Verlag London, 2001.
- [33] G. M. VAN DE VEN AND A. S. TOLIAS, *Three scenarios for continual learning*, arXiv preprint arXiv:1904.07734, (2019).
- [34] X. WAN AND G. E. KARNIADAKIS, *Multi-element generalized polynomial chaos for arbitrary probability measures*, SIAM Journal on Scientific Computing, 28 (2006), pp. 901–928.
- [35] S. WEISBERG, *Applied linear regression*, vol. 528, John Wiley & Sons, 2005.
- [36] Z. ZOU AND G. E. KARNIADAKIS, *L-HYDRA: Multi-Head Physics-Informed Neural Networks*,

arXiv preprint arXiv:2301.02152, (2023).

- [37] Z. ZOU, X. MENG, A. F. PSAROS, AND G. E. KARNIADAKIS, *NeuralUQ: A comprehensive library for uncertainty quantification in neural differential equations and operators*, arXiv preprint arXiv:2208.11866, (2022).

Appendix A. Details of the methodology.

A.1. Algorithm for deleting one data point. Here, we provide details for the algorithm for deleting one data point from Section 4.2. Removing the j -th data point corresponds to removing the term $\frac{1}{2}\lambda_j\|\Phi_j\boldsymbol{\theta} - \mathbf{y}_j\|_2^2$ in the loss function (4.1) or, equivalently, removing the Hamiltonian $\frac{1}{2}\|\Phi_j\boldsymbol{\theta} - \mathbf{y}_j\|_2^2$ from the multi-time HJ PDE and removing the pieces $L_j(s, \mathbf{u}) = \frac{1}{2}\mathbf{u}^T\mathbf{u} - \mathbf{y}_j$ and $f(s, \mathbf{u}) = \Phi_j^T\mathbf{u}$ from the running cost and dynamics, respectively, of the corresponding piecewise LQR problem. Hence, numerically, we can remove the j -th data point by solving the following Riccati ODE

$$(A.1) \quad \begin{cases} \dot{\tilde{P}}(t) = -\tilde{P}(t)^T\Phi_j^T\Phi_j\tilde{P}(t) & t < \lambda_j, \\ \dot{\tilde{\mathbf{q}}}(t) = -\tilde{P}(t)^T\Phi_j^T(\Phi_j\tilde{\mathbf{q}}(t) - \mathbf{y}_j) & t < \lambda_j, \end{cases}$$

with terminal condition $\tilde{P}(\lambda_j) = P(T_N)$ and $\tilde{\mathbf{q}}(\lambda_j) = \mathbf{q}(T_N)$, where $P(T_N)$ and $\mathbf{q}(T_N)$ are obtained from solving the learning problem (4.1) with all N data points. Then, the solution to the new learning problem with the j -th point removed is given by (4.4), where $\tilde{P} = \tilde{P}(0)$ and $\tilde{\mathbf{q}} = \tilde{\mathbf{q}}(0)$ are the solution to (A.1).

A.2. Algorithm for tuning the regularization weights. Here, we provide details for the algorithm for deleting one data point from Section 4.3. We consider the case where we change each regularization parameter γ_k to $\tilde{\gamma}_k$. This change can be regarded as two steps: first, we change all parameters γ_k for the indices k such that $\tilde{\gamma}_k > \gamma_k$, and then we change the other parameters. Define the index set \mathcal{K} to be $\mathcal{K} = \{k: \tilde{\gamma}_k > \gamma_k\}$.

The first step is equivalent to adding the term $\sum_{k \in \mathcal{K}} \frac{\tilde{\gamma}_k - \gamma_k}{2} (\theta_k - \theta_k^0)^2$ to the loss function (4.1). We can interpret this as adding an $(N+1)$ -th Hamiltonian $\frac{1}{2}\boldsymbol{\theta}^T\Gamma_+\boldsymbol{\theta}$ with corresponding time variable $t_{N+1} = 1$ to the multi-time HJ PDE, where Γ_+ is a diagonal matrix whose k -th diagonal element is $\tilde{\gamma}_k - \gamma_k$ if $k \in \mathcal{K}$ and 0 otherwise. Therefore, the solution to this new multi-time HJ PDE can be solved by the following Riccati equation:

$$(A.2) \quad \begin{cases} \dot{P}_+(t) = -P_+(t)^T\Gamma_+P_+(t) & t \in (0, 1), \\ \dot{\mathbf{q}}_+(t) = -P_+(t)^T\Gamma_+\mathbf{q}_+(t) & t \in (0, 1), \end{cases}$$

with initial condition $P_+(0)$ and $\mathbf{q}_+(0)$, which are the corresponding solutions to the Riccati equations before changing the weights $\gamma_k, k \in \mathcal{K}$. In other words, we set $P_+(0) = P(T_N)$ and $\mathbf{q}_+(0) = \mathbf{q}(T_N)$, where $P(T_N), \mathbf{q}(T_N)$ are obtained from solving the original learning problem (4.1) with the original values of γ_k .

The second step is equivalent to removing the term $\sum_{k \notin \mathcal{K}} \frac{\gamma_k - \tilde{\gamma}_k}{2} (\theta_k - \theta_k^0)^2$ from the loss function (4.1). This is equivalent to solving a single-time HJ PDE with a terminal condition at time 1 and Hamiltonian $\frac{1}{2}\boldsymbol{\theta}^T\Gamma_-\boldsymbol{\theta}$, where Γ_- is a diagonal matrix whose k -th diagonal element is $\gamma_k - \tilde{\gamma}_k$ if $k \notin \mathcal{K}$ and 0 otherwise. Then, the solution can be obtained by solving the following Riccati equation:

$$(A.3) \quad \begin{cases} \dot{P}_-(t) = -P_-(t)^T\Gamma_-P_-(t) & t \in (0, 1), \\ \dot{\mathbf{q}}_-(t) = -P_-(t)^T\Gamma_-\mathbf{q}_-(t) & t \in (0, 1), \end{cases}$$

with terminal condition $P_-(1) = P_+(1)$ and $\mathbf{q}_-(1) = \mathbf{q}_+(1)$, where P_+, \mathbf{q}_+ are obtained from the solution to (A.2).

Finally, the minimizer of the new learning problem after changing all of the weights γ_k in the regularization term is given by $P_-(0)\tilde{\Gamma}\boldsymbol{\theta}^0 + \mathbf{q}_-(0)$, where P_-, \mathbf{q}_- are obtained from the solution to (A.3) and $\tilde{\Gamma}$ is a diagonal matrix whose k -th diagonal element is the new regularization parameter $\tilde{\gamma}_k$.

Appendix B. Additional results for example 2. In Section 5.2, we consider a 1D steady-state linear reaction-diffusion equation and discuss three different types of post-training calibrations: adding new data points to compensate for a lack of knowledge in the regular training, enforcing the fitting of some data points by increasing the weights λ_i of their respective terms in the loss function (5.4), and removing some data points so that their effects are eliminated. In this section, we present the results for the last case. In Figure 9, we remove two outliers one-by-one and observe that their removal does successfully increase the accuracy of the learned model. Again, using our Riccati-based approach, the removal of these points is done using only knowledge about the point to be removed and the results of the previous training step.

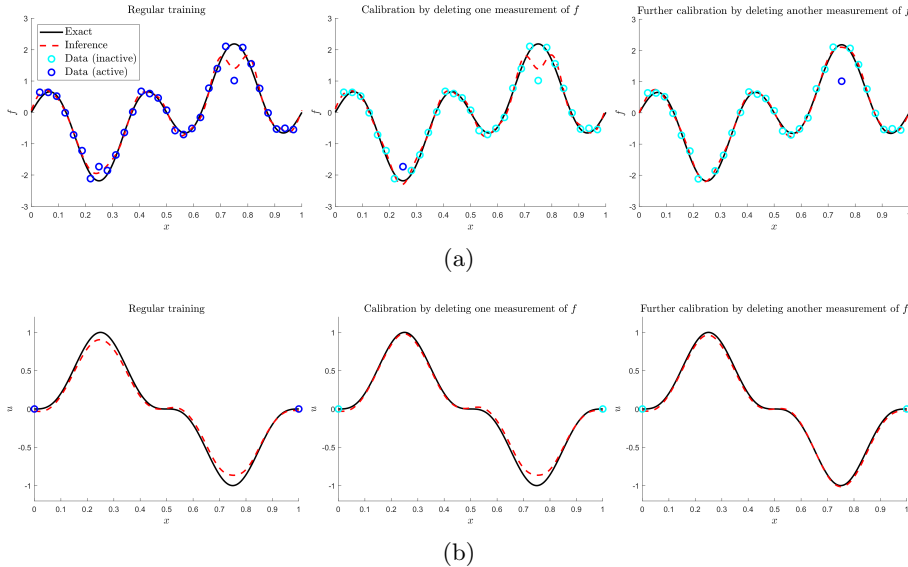


Fig. 9: Results of solving the 1D steady-state reaction-diffusion equation (5.3) with noisy measurements of the source term f in the domain and noiseless measurements of the solution u on the boundary. (a) results for f ; (b) results for u . **Left:** results of regular training using our Riccati-based method in Section 4.1; **middle and right:** calibrating the results of regular training by eliminating two outlier measurements of f using the methodology described in Section 4.2. Calibrations are employed without re-training or access to the data from the previous training.